Hydrol. Earth Syst. Sci. Discuss., https://doi.org/10.5194/hess-2018-260
Manuscript under review for journal Hydrol. Earth Syst. Sci.
Discussion started: 31 May 2018

Hydrology and Earth System Sciences
Open Access
Discussions

Multi-scale temporal variability in meltwater contributions in a tropical glacierized watershed

Leila Saberi[1], Rachel T. McLaughlin[1], G.-H. Crystal Ng[1,2], Jeff La Frenierre[3], Andrew D. Wickert[1,2], Michel Baraer[4], Wei Zhi[5], Li Li[5], and Bryan G. Mark[6]

[1]Department of Earth Sciences, University of Minnesota - Twin Cities, Minneapolis, MN 55455, USA
[2]Saint Anthony Falls Laboratory, University of Minnesota - Twin Cities, Minneapolis, MN 55455, USA
[3]Department of Geography, Gustavus Adolphus College, St. Peter, MN 56082, USA
[4]Construction Engineering, École de Technologie Supérieure, Université du Quebec, Montreal, Canada H3C 1K3
[5]Department of Civil & Environmental Engineering, Pennsylvania State University, University Park, PA 16802-1294, USA
[6]Department of Geography, The Ohio State University, Columbus, OH 43210-1361, USA

Correspondence: Leila Saberi (saber017@umn.edu)

Abstract. Climate models predict amplified warming at high elevations in low latitudes, making tropical glacierized regions some of the most vulnerable hydrological systems in the world. Observations reveal decreasing streamflow due to retreating glaciers in the Andes, which hold 99% of all tropical glaciers. However, the timescales over which meltwater contributes to streamflow and the pathways it takes – surface and subsurface – remain uncertain, hindering our ability to predict how shrinking glaciers will impact water resources. Two major contributors to this uncertainty are the sparsity of hydrologic measurements in tropical glacierized watersheds and the complication of hydrograph separation where there is year-round glacier melt. We address these challenges using a multi-method approach that employs repeat hydrochemical mixing model analysis, hydroclimatic time series analysis, and integrated watershed modeling. Each of these approaches interrogates distinct timescale relationships among meltwater, groundwater, and stream discharge. Our results challenge the commonly held conceptual model that glaciers buffer discharge variability. Instead, in a sub-humid watershed on Volcán Chimborazo, Ecuador, meltwater drives nearly all the variability in discharge (Pearson correlation coefficient of 0.89 in simulations), with glaciers contributing a broad range of 20-60% or wider of discharge, mostly (86%) through surface runoff on hourly timescales, but also through infiltration that increases annual groundwater contributions by nearly 20%. We further found that rainfall may enhance melt contributions to discharge at timescales that complement melt generation, possibly explaining why minimum discharge occurred at the study site during warm but dry El Niño conditions, which typically heighten melt in the Andes. Our findings caution against extrapolations from isolated measurements: stream discharge and meltwater contributions in tropical glacierized systems can change substantially at hourly to interannual timescales, due to climatic variability and surface to subsurface flow processes.

1 Introduction

Glaciers supply water resources to over 600 million people worldwide (Messerli et al., 2004). By melting during dry seasons and drought years, they supplement streamflow (Fountain and Tangborn, 1985; Lang, 1986; Escher-Vetter et al., 1994; Jansson et al., 2003; Juen et al., 2007; Soruco et al., 2015; Chen et al., 2017) and ensure reliable water supplies (Mark and Seltzer, 2003; Mark and Mckenzie, 2007; Bury et al., 2013). This has led to the commonly held conceptual model, called the "glacier compensation effect" (Lang, 1986), in which meltwater buffers discharge variability.

Climate change can disrupt the glacier compensation effect, and tropical glacierized watersheds that already experience year-round melt (Kaser and Osmaston, 2002) may be the most vulnerable. Climate models predict amplified temperature increases at high altitudes in low latitudes (Bradley, 2006; Pepin et al., 2015). The retreat of these glaciers temporarily results in increased runoff (Braun et al., 2000; Mark, 2008; Polk et al., 2017; Carey et al., 2017), but gradually depletes the storage of these mountain "water towers". Over time, this reduction in storage capacity can render these glaciers unable to supply sufficient dry-season meltwater discharge for the communities that depend on it (Barnett et al., 2005; Bradley, 2006; Mackay, 2008; Ostheimer et al., 2005; Luce, 2018). Indeed, observations already reveal reduced and fluctuating flows in glacierized watersheds (Mark and Seltzer, 2003; Huss et al., 2008; Baraer et al., 2012; Rabatel et al., 2013; Baraer et al., 2015; Soruco et al., 2015), threatening the water security of millions of people (Carey et al., 2017; Immerzeel et al., 2010; Vuille et al., 2018).

Of all glaciers in the tropics, 99% are located in the Andes (Kaser, 1999), often in remote regions, where resource-limited populations often rely on their meltwater (Bury et al., 2011; La Frenierre and Mark, 2017). Despite over a decade of research conducted in Peru's heavily glacierized Cordillera Blanca (Mark and Seltzer, 2003; Mark and Mckenzie, 2007; Juen et al., 2007; Mark et al., 2005; Baraer et al., 2012, 2015), many of the processes linking variability in climate, glacier melt, and stream discharge remain uncertain. For example, groundwater is also a major contributor to discharge in many glacierized mountainous watersheds around the world (Tague et al., 2008; Tague and Grant, 2009; Andermann et al., 2012; Baraer et al., 2015; Markovich et al., 2016; Engel et al., 2016; Schmieder et al., 2018). This can further modulate discharge through baseflow (Jasechko et al., 2016; Staudinger et al., 2017). However, its capacity to do so as glaciers respond to climate change is complicated by largely unconstrained relationships between glacial meltwater and groundwater recharge (Favier et al., 2008a; Baraer et al., 2015; Gordon et al., 2015).

Understanding how different surface and subsurface pathways influence the timing of meltwater and groundwater contributions to streamflow is critical for predicting how climate change will impact the reliability of watershed discharge. A major challenge in evaluating these spatiotemporal effects in tropical glacierized watersheds is the relative data sparsity and resource limitations in these regions when compared to better instrumented mountainous systems in North America and Europe. Because of these constraints, many studies in tropical and other remote glacierized settings rely on focused field campaigns using methods such as synoptic water chemistry tracer sampling (Mark and Mckenzie, 2007; Baraer et al., 2009, 2015; Wilson et al., 2016), but these provide only snapshots of the hydrologic state. Even though physically based hydrologic models can provide greater spatiotemporal coverage in mountainous settings (e.g., Suecker et al., 2000; Liu et al., 2004; Tague et al., 2008; Tague and Grant, 2009; Lowry et al., 2010, 2011; Markovich et al., 2016; Pribulick et al., 2016; Omani et al., 2017; He et al., 2018), their application is relatively limited in most Andean watersheds (implementations include work by Buytaert and Beven, 2011; Minaya, 2016; Omani et al., 2017; Ng et al., 2018) due to the lack of extensive monitoring infrastructure. With these obstacles, there remains limited understanding of how stream discharge in tropical glacierized watersheds varies over time scales ranging from hours to years, and how this variability is driven by dynamic inputs of glacial meltwater and precipitation through a combination of surficial and subsurface pathways.

In this study, we probe the multiple time scales of hydrological processes in a sub-humid glacierized watershed on Volcán Chimborazo in the tropical Ecuadorian Andes. Prior to this work, there have been no comprehensive efforts on Chimborazo to quantify glacier melt as a component of watershed discharge. In contrast to the well-studied crystalline-cored Cordillera Blanca in the outer tropics, Chimborazo is a stratovolcano located in the inner tropics, and therefore experiences less-pronounced seasonality in precipitation (Kaser and Osmaston, 2002) and more persistent ablation due to higher humidity (Vuille et al., 2003; Favier, 2004; Harpold and Brooks, 2018). Most mixing model analyses of melt contributions in the outer tropics have been limited to the dry season, leaving wet season effects less well understood. In the inner tropics, coincident glacier melt and precipitation inputs throughout the year could lead to multiple processes simultaneously driving discharge variability – likely at diverse timescales – that are difficult to disentangle. Furthermore, Andean volcanoes may feature fractured bedrock aquifers that support greater groundwater storage and baseflow than those in crystalline-cored mountainous watersheds (Tague and Grant, 2009; Markovich et al., 2016), adding another factor to be reconciled. A growing body of work at Volcán Antisana, also located in the inner tropics, has begun to shed light on its hydrogeologic (Favier, 2004; Caceres et al., 2006; Favier et al., 2008b; Cauvy-Fraunié et al., 2013) and ecohydrologic (Minaya, 2016) conditions, but comprehensive understanding of mountain hydrology in the inner tropics still greatly lags that in the outer tropics.

Here, we implement diverse field and computational methods to answer two questions: (1) What is the temporal variability of relative meltwater contributions to discharge, from hourly to multi-year time scales, in a sub-humid glacierized watershed on Volcán Chimborazo? (2) What hydroclimatic factors control this variability? Our approach comprises three methods: mixing model analysis applied to repeat synoptic sampling, time series analysis of hydroclimatic data, and numerical watershed modeling. Each method interrogates a distinct temporal relationship, and synthesizing their results illuminates how the dominant surface and subsurface processes driving the hydrological response of a tropical glacierized watershed vary as a function of time scale.

2 Study Area

Volcán Chimborazo is a glacierized stratovolcano in Ecuador (Figure 1(a)) whose glaciers serve as the headwaters for four major river systems that supply water to a population of over 200,000 (INEC, 2010). Located in the inner tropics, Chimborazo's climate is characterized by minimal intra-annual temperature variation ($\sim$2°C) and moderately seasonal precipitation, with two wetter seasons of unequal length (February-May and October-November) (Clapperton, 1990), and two intervening drier seasons that have less but not negligible amounts of precipitation. Moisture mostly originates from the Amazon Basin to the east (Vuille and Keimig, 2004; Smith et al., 2008), which produces a steep northeast (up to 2000 mm/yr) to southwest (<500 mm/yr) precipitation gradient across the mountain (Clapperton, 1990). Driving interannual climatic variability at the regional scale, El Niño generally brings drier and hotter conditions throughout the Andes (Vuille and Bradley, 2000; Wagnon et al., 2001; Francou, 2003; Bradley et al., 2003; Vuille and Keimig, 2004; Smith et al., 2008), which enhances glacier ablation (Wagnon et al., 2001; Favier, 2004; Veettil et al., 2014b).

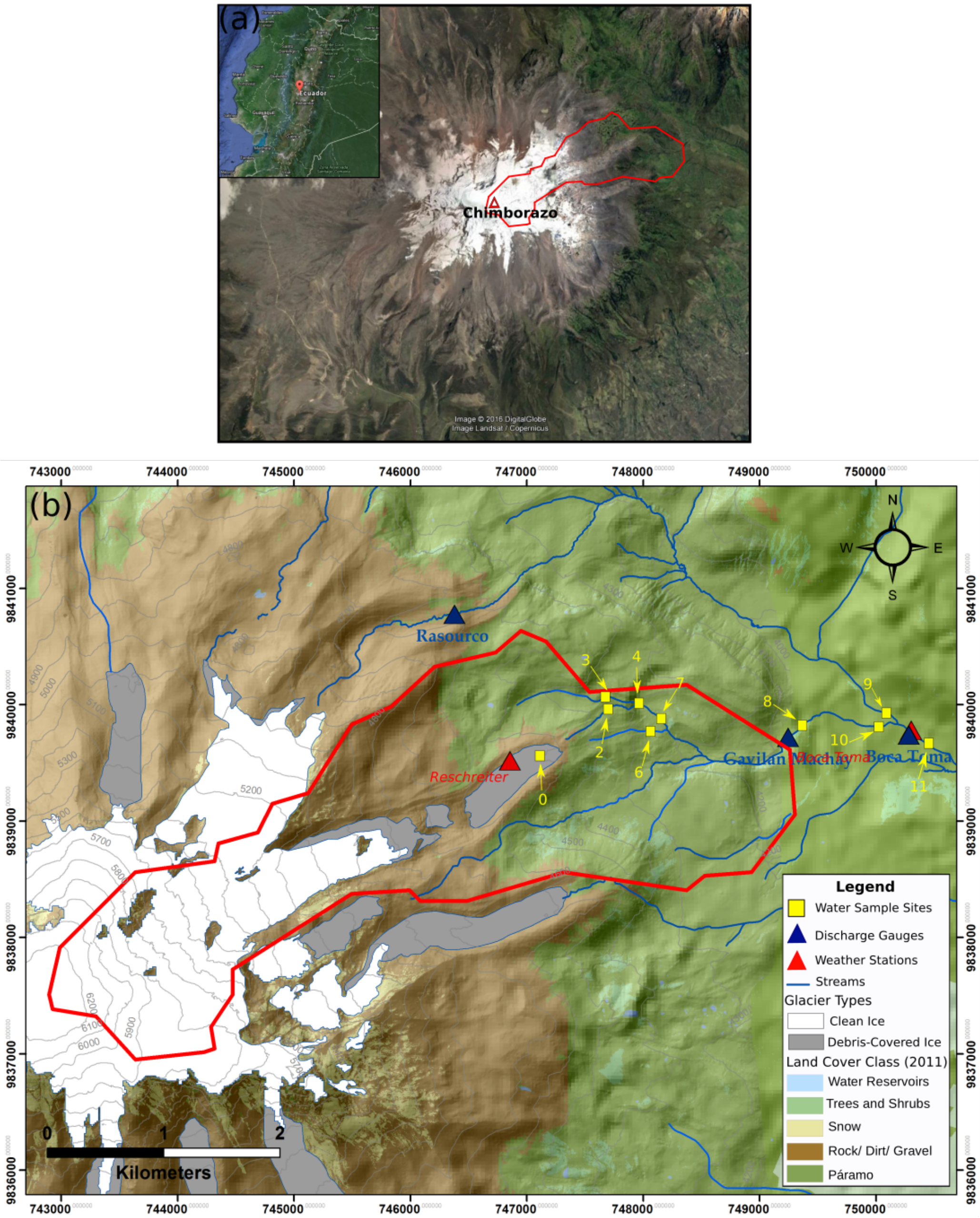

Figure 1. (a) Satellite image of Volcán Chimborazo, with the study watershed Gavilan Machay outlined in red, and its location in Ecuador shown in the inset map. The glacierized Gavilan Machay watershed is a relatively humid watershed compared to the western flanks of Chimborazo. **(b)** Land cover and monitoring station and water sample locations within the Gavilan Machay watershed.

Records since 1980 indicate that, consistent with the rest of the tropical Andes, temperatures have warmed 0.11°C decade^{-1} around Volcán Chimborazo (Vuille et al., 2008; La Frenierre and Mark, 2017). This likely caused the 21% reduction in ice area since 1986 (La Frenierre and Mark, 2017). Although regional precipitation gauges show no notable change over time, local residents report a reduction in precipitation, which could further drive glacier mass balance changes (La Frenierre and Mark, 2017). Under current conditions, only four of Chimborazo's seventeen glaciers, including the two largest, Reschreiter (2.55 km^2) and Hans Meyer (1.33 km^2), generate perennial surface discharge, nearly all of which flows northeast into the Río Mocha watershed. The lowest 16% of Reschreiter Glacier is debris-covered, providing insulation that stabilizes ice at lower elevations (4480 m.a.s.l) than would be expected for clean ice, given current climatic conditions. Our study focuses on the 7.5 km^2 Gavilan Machay sub-catchment on the sub-humid northeast flanks of Chimborazo (Figure 1(b)), which is 34% glacierized by Reschreiter and is of concern because it discharges into the main Río Mocha channel just upstream of the Boca Toma diversion point (3895 m.a.s.l. elevation) for an irrigation system.

In addition to glacier melt, groundwater and ecological conditions also control the hydrology of the Gavilan Machay watershed. Springs are prevalent below 4400 m.a.s.l. Geologic maps and stratigraphic interpretations (Barba et al., 2005; Samaniego et al., 2012) support field evidence for aquifers within unsorted glacial deposits and underlying fractured bedrock (McLaughlin, 2017). Extensive areas of páramo, the biologically rich grasslands endemic to the tropical Andes above ∼3500 m.a.s.l., are common across the watershed. Wet páramos commonly contain homogeneous Andosol soils of volcanic origin that can accumulate elevated organic carbon content; this typically gives rise to high porosity, infiltration capacity, hydraulic conductivity, and water retention (Buytaert et al., 2006; Buytaert and Beven, 2011). Absorbent páramo soils are considered to very efficiently regulate watershed discharge throughout Andean Ecuador (Buytaert et al., 2006; Buytaert and Beven, 2011; Minaya, 2016).

3 Methods

3.1 Hydroclimatic Data

Precipitation, temperature, and relative humidity data were collected from October 2011 to February 2017 from weather stations installed at 4515 m.a.s.l on the debris-covered portion of Reschreiter Glacier and at 3895 m.a.s.l. at Boca Toma (Figure S1). The Boca Toma weather station was deployed with an Onset Hobo Pendant® Event Logger starting June 16, 2015. The Reschreiter weather station was deployed with an Onset Hobo Micro Station starting October 2011, but temperature and precipitation data recovery was discontinuous. The short data records from Reschreiter were primarily used together with Boca Toma data to determine lapse rates for precipitation. In June 2016, glacier ablations stakes were installed at two elevations on the Reschreiter Glacier tongue (4792 and 4820 m.a.s.l.) and one on the Hans Meyer Glacier tongue (4925 m.a.s.l.). Each stake included a temperature sensor, along with a look-down ultrasonic sensor for measuring changes in distance to the ice surface to estimate glacier mass loss. The stakes were deployed using the open-source Arduino-based ALog data logger (Wickert, 2014). All sensors were mounted at the top of 3 m long PVC tubes, which were inserted into holes drilled to about 2.5 m depth. Temperature lapse rates were calculated using data collected on the glacier ablation stakes over June 2016 to November 2016. We obtained unmeasured meteorological variables (wind speed, solar radiation, longwave radiation, and air pressure) from the

Global Land Data Assimilation Systems (GLDAS) (Rodell et al., 2004). A discharge gauging station equipped with a Solinst Levelogger Junior pressure transducer was established at Gavilan Machay, 1.1 km upstream of the Río Mocha confluence. Solinst Barologger measurements at Boca Toma were applied to correct for atmospheric pressure, and standard USGS rating curve techniques (Andrews, 1981a, b) were used to convert water depth to discharge over the period of record (Figure S1).

3.2 Hydrochemical and Isotopic Tracers

3.2.1 Field Sampling

Water samples were collected for use in the Hydrochemical Basin Characterization Model (HBCM) (details in Section 3.3), a hydrochemical mixing model that spans the stream network and requires synoptic water sampling over a sufficiently short time period such that data reflect spatial and not temporal variability. We carried out five synoptic sampling campaigns during January 1-8, 2012; July 7-9, 2012; June 12-15, 2015; June 25-30, 2016; and February 4-7, 2017. The June and July (January and February) samples represent the longer (shorter) dry season. In addition to limiting the number of sampling days, synoptic sampling should avoid hourly timescale hydrochemical fluctuations. All samples were collected between mid-morning and mid-afternoon. In February 2017, we confirmed that 1-minute resolution specific conductivity changes over a 24-hour time period at the Reschreiter glacier tongue were an order of magnitude smaller than the spatial variability across the Gavilan Machay subcatchment (details in McLaughlin, 2017). Logistical difficulties prevented similar measurements farther downstream in the watershed, where dynamic melt versus groundwater contributions likely caused greater hydrochemical variability (discussed further in Section 4.1).

During each of the five campaigns, we collected water samples from glacial meltwater, springs, and precipitation (locations shown in Figure 1(b)), as well as at stream confluence mixing points. Spring samples from concrete capture boxes or natural valley wall seeps represent groundwater, which consists of an unconstrained mix of shallow saturated soil water from páramo areas, morainic debris aquifer water, and deeper fractured bedrock aquifer water. Precipitation samples were collected using evaporation-proof totalizing rain gauges deployed for 3-6 days at Boca Toma, near the Reschreiter weather station, and near Hans Meyer glacier (at 4780 m.a.s.l.). Each field campaign covered most of the same sampling locations between the Reschreiter glacier tongue and the Gavilan Machay confluence. The 2012 and 2017 sampling periods included additional stream samples between some confluences to estimate groundwater contributions along shorter stream reaches (schematics in Figure 2(b)). For each sampling site, 30mL of water were collected, filtered in the field using either 0.45 μm (before 2017) or 0.2 μm (2017) filters, and stored in Nalgene bottles that were capped and sealed with electrical tape, and then stored near 4°C as soon as possible.

3.2.2 Laboratory Analysis

In 2012, major dissolved ions (Li$^+$, Na$^+$, K$^+$, Mg^{2+}, Ca^{2+}, F$^-$, Cl$^-$, NO$_3^-$, PO$_4^{3-}$ and SO$_4^{2-}$) were measured using a Dionex DX500 Ion Chromatographer at the Water Isotope and Nutrient Laboratory at The Ohio State University, and stable isotopes of water (δ18O and δ2H) were measured using Piccaro L2130-i CRDS isotope analyzers at the Water Isotope and Nutrient Laboratory

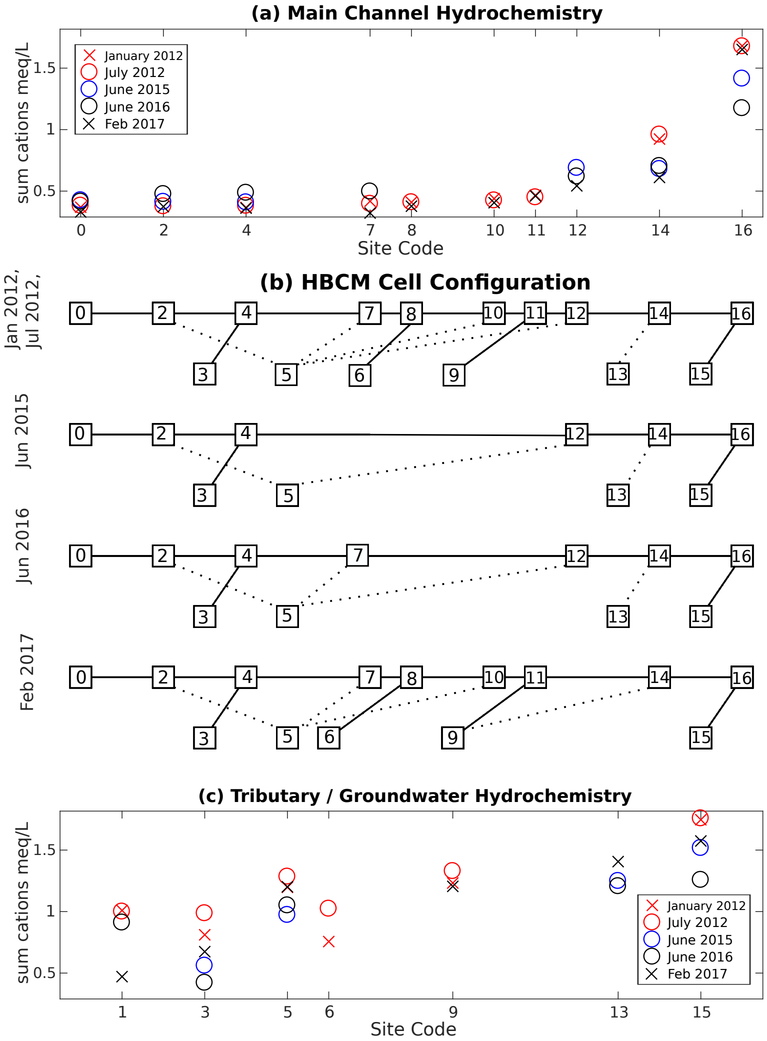

Figure 2. **(a)** Hydrochemistry at different sampling locations along the Gavilan Machay main channel shows variability in space and over the five sampling periods; site codes are ordered from highest (0 for meltwater) to lowest (16 for Boca Toma) elevation (see Figure 1(b)). **(b)** Different computational cell configurations for the HBCM mixing model based on the available samples (site codes in squares) for each of the five periods. The upper solid lines for each period represent the main channel. The lower solid lines depict tributary links for confluence cells, and the lower dotted lines show groundwater inputs to the main channel for reach cells. **(c)** Hydrochemistry for different tributary and groundwater (spring) samples, ordered from highest to lowest elevation, show variability in space and time.

and at the Byrd Polar Research Center. In 2015-2017, cations (Na^+, K^+, Mg^{2+}, Ca^{2+}) were measured using an Agilent 7700X Inductively Coupled Plasma-Mass Spectrometer (ICP-MS) at Gustavus Adolphus College, anions (F^-, Cl^-, SO_4^{2-}) were measured using a Dionex ICS1000 Ion Chromatographer (IC) also at Gustavus Adolphus College, and stable isotopes of water ($\delta^{18}O$ and δ^2H) were measured at the University of Minnesota using an LGR DLT-100 Liquid Water Analyzer (a laser spectroscopy system). We calculated the bicarbonate (HCO_3^-) concentration as the charge balance residual. Reported isotope ratios are relative to the Vienna Standard Mean Ocean Water (VSMOW) and typical precisions are ±1.0‰ for deuterium/hydrogen values and ±0.25‰ for $^{18}O/^{16}O$ values.

3.2.3 Mixing Model: Hydrochemical Basin Characterization Model (HBCM)

Naturally occurring dissolved ions and stable isotopes of water ($\delta^{18}O$ and δ^2H) have long been used to track the relative contributions of different surface source waters to total watershed discharge (Hooper and Shoemaker, 1986; Mark and Seltzer, 2003; Ryu et al., 2007; Mark and Mckenzie, 2007; Baraer et al., 2009), as well as to identify groundwater flow paths (Clow et al., 2003; Kendall et al., 2003; Baraer et al., 2009; Crossman et al., 2011; Baraer et al., 2015). Here, the proportion of glacier melt versus groundwater in discharge at the Gavilan Machay watershed is quantified using the Hydrochemical Basin Characterization Model (HBCM), a multi-component hydrochemical mixing model developed for use in data-sparse, glacierized tropical watersheds (Baraer et al., 2009). Given source (or "end-member") and outflow chemistries at different mixing points throughout the watershed, HBCM solves an over-constrained set of mass balance equations for multiple tracers (ion concentrations or stable water isotope values) to determine the relative flow contributions of each source. Details are provided in the Supplementary Information (HBCM Section).

As with all hydrochemical mixing models, HBCM's calculation of relative source contributions depends on three fundamental assumptions: (1) end-member chemistry is be unique and spatially homogeneous within the analysis area, (2) tracers are chemically conservative within the analysis, and (3) end-member mixing is instantaneous and complete (Christophersen et al., 1990; Soulsby et al., 2003). A unique feature of HBCM is that it represents spatial information within a watershed through a series of cells that are interconnected by having outflow from one become inflow to a subsequent downstream cell. There are two types of cells, both of which have streamflow at the upgradient end of the cell as a source and streamflow at the downgradient end of the cell as the mixed water output. "Reach cells" have groundwater as their other source, and "confluence cells" have tributary water as their other source (see cartoon in Figure S2). Note that this makes end-members for a particular HBCM cell different than for the full watershed, which has only meltwater and groundwater as sources contributing to discharge at the outlet. Figure 2b shows the conceptual schematics of Gavilan Machay cell configuration for the five sampling periods.

Although HBCM only requires the three assumptions to be met on a cell-scale, we carried out a preliminary watershed-level analysis considering groundwater and meltwater as sources to all mixed stream samples, in order to identify potential conservative tracers that are reasonable candidates for all cells. Appropriate tracers should show end-members appearing on opposite ends of a line formed by mixed samples in bivariate plots, and samples for different end-members should group separately from each other in hierarchical cluster analysis diagrams (Christophersen et al., 1990; Hooper, 2003; James and

Roulet, 2006). Stable isotopes were excluded as tracers for reach cells, because the groundwater likely has a range of isotopic values due to different recharge elevations.

To bracket some of the uncertainty in the method, HBCM generates estimates of fractional contributions from each source using different combinations of potential tracers. The final result consists of a range of estimates that produce similar (within about three times the minimum) cumulative residual errors between the measured tracer concentrations in the mixed outflow water and that predicted by the over-constrained mixing model. This quantifies uncertainty due to the model's inability to distinguish among equally good optimization results, but it should be noted that this represents only a lower limit of error, because it does not account for the mismatch between the observed and predicted mixed concentration outflows. There are no straightforward methods to convert the sum of residual concentration flux errors to estimated source contribution errors.

3.3 Integrated Hydrologic Modeling

Spatially distributed watershed models can integrate surface hydrology and groundwater flow through time to evaluate their joint impacts on water resources. Over the one-year period of June 2015-June 2016 when continuous air temperature and precipitation measurements are available in the watershed, we implement Flux-PIHM (Shi et al., 2013), an intermediate complexity watershed model that balances mechanistic parameterizations with computational efficiency. Full details about Flux-PIHM can be found in Qu and Duffy (2007) and Shi et al. (2013); here, we summarize the major features. Flux-PIHM couples physically based equations for canopy interception, infiltration, surface and subsurface water flow, and snow melt with the energy balance scheme of the NOAH land-surface model (Ek et al., 2003) for more accurate simulation of evapotranspiration. Flux-PIHM employs a semi-discrete finite volume approach on an unstructured grid that performs efficiently on steep topographies. Channel and overland flow are represented by diffusion wave approximations to St. Venant equations; shallow groundwater flow follows a 2-D Dupuit approximation; and unsaturated zone flow is based on a 1D form of Richards equation. The model simulates water storage in one vertically integrated unsaturated zone layer and one vertically integrated saturated zone layer, providing a "2.5D" distributed model.

Flux-PIHM calculates snowmelt based on energy balance. We added another module to simulate glacier melt using a temperature-index (TI) scheme (NRCS, 2009):

$$F_I = M_I(T_a - T_{M,I}) \qquad T_a > T_{M,I} \tag{1a}$$

$$F_I = 0 \qquad\qquad T_a < T_{M,I} \tag{1b}$$

where F_I is the ice melt rate (m/hr), Ta is air temperature in the grid cell containing ice (°C), M_I is the melt factor parameter (m/hr/°C), and $T_{M,I}$ (°C) is set to 0°C as the air temperature threshold for ice to melt. Over the simulated time period, we assume that there is an unexhausted supply of ice that can melt in the glaciated grid cells below the equilibrium line altitude at 5050 m.a.s.l. (Frenierre and Mark, 2014), which is a reasonable approximation over the one-year simulation period. The accuracy of a temperature index glacier melt model for tropical glaciers can be uncertain due to uncaptured effects of solar radiation, cloud cover, humidity, topography, and aspect (Hock, 1999, 2005; Pellicciotti et al., 2005; Sicart et al., 2008; Huss et al., 2009; Gabbi et al., 2014; Fernández and Mark, 2016). However, it remains the most feasible approach to estimate melt in poorly instrumented watersheds given its simplicity and limited field data requirement compared to an energy balance approach (Hock, 2005; Fernández and Mark, 2016; Reveillet et al., 2017). The melt simulated with the temperature index model was added to the precipitation amount for the Flux-PIHM forcing inputs.

We used the PIHMgis software (Bhatt et al., 2014) to construct an unstructured domain of 188 cells over the Gavilan Machay subcatchment using a 30 m resolution Shuttle Radar Topography Mission (SRTM) Digital Elevation Model (DEM) (Farr et al., 2007). Although a major feature of PIHMgis is its tight integration with spatial and temporal datasets for model inputs such as soil properties and meteorological forcing, these datasets only cover densely monitored regions, mostly within North America and Europe. For meteorological forcing, we used spatially distributed temperature, precipitation and relative humidity measured and interpolated in the watershed, along with incoming shortwave and longwave radiation, wind speed, and air pressure obtained from the corresponding GLDAS grid cell. Vegetation mapping by McLaughlin (2017), based on 30-cm resolution aerial photo surveys conducted by the Sistema Nacional de Información de Tierras Rurales e Infrastructura Tecnológica (SIGTIERRAS; http://www.sigtierras.gob.ec/descargas/), provided land-cover types and boundaries. Built-in land-cover parameters from Noah-LSM were used for the “grassland/herbaceous” type at lowest elevations corresponding to páramo, the “barren/sparsely vegetated” type for intermediate elevations with rock/dirt/gravel, and the “perennial ice/snow” type for the ice-covered areas. This approach simplifies the mix of tussock grasses, acaulescent rosettes, and cushion plants that make up the páramo into a single representative “grassland/herbaceous” type in order to reduce the calibration burden. For the grassland/herbaceous land cover type, the default monthly Leaf Area Index (LAI) values were replaced with measurements from MODIS (Vermote, 2015) to avoid using incorrect seasonal changes from the original model settings for this tropical region. Hydraulic parameters were manually calibrated to match observed discharge at Gavilan Machay.

4 Results and Discussion

This section presents the respective insights gained from each of the three methods on the temporal relationship among meltwater, groundwater, and discharge: the mixing model analysis offers discrete multi-year estimates over five years, the time series analysis shows fine-scale hourly resolution correlations, and the integrated hydrological model explores intermediary weekly to seasonal processes within a one-year simulation period containing a strong El Niño event. A complete interpretation of the multi-scale temporal variabilities and their hydroclimatic controls emerges in Section 4.3.2 when evaluating the model simulations in relation to the mixing model and time series analysis results.

4.1 Mixing-model analysis of meltwater contributions to discharge

Total cation concentrations provide a summary representation of hydrochemistry results from the five dry-season synoptic sampling periods in Figure 2(a) and (c). These plots show that even though hydrochemical conditions vary over the different periods, groundwater samples, which geochemically interact with soil and rocks, consistently contain much higher ion concentrations than meltwater samples, which are relatively solute-free. The distinctive chemistries of groundwater and meltwater make it possible to use the mixing model approach to estimate their relative contributions to streamwater, which shows an increase in ion concentration while moving downgradient due to the cumulative addition of groundwater (see Figure 1(b) for sample locations). Bivariate plots of specific hydrochemical constituents (Figures S3-S7) support the selection of the following potential tracers: sum of monovalent cations, Mg^{2+}, Ca^{2+}, Cl^-, and HCO_3^-. Hierarchical cluster analysis lends confidence that these five potential tracers can be used in the mixing model analysis to distinguish between groundwater and melt samples as different watershed-level end-members (Figure S8). Precipitation was not included as an end-member, because precipitation samples tended to plot outside the range of stream samples bracketed tightly by groundwater and meltwater samples in bivariate plots. Rather than directly add to streamflow, any precipitation that fell close to the sampling time likely evapotranspired or infiltrated and contributed to streamflow through groundwater.

HBCM results in Figure 3 illustrate the importance of both meltwater and groundwater in the watershed. Surficial meltwater comprises between 23-66% of discharge during the five dry-season sampling periods, with groundwater constituting the remaining 34-77% at any given time. Notable differences were observed across the sampling periods. The higher melt fraction during February 2017 compared to January 2012 could reflect the accelerating melt rates observed on Chimborazo (La Frenierre and Mark, 2017). However, the absolute contribution, determined by applying estimates of melt fractions to average observed weekly discharge measurements around the sampling time, was lowest in February 2017, because of significantly less groundwater discharge compared to the other sampling periods (Figure 3(b)). Our findings across the five sampling periods demonstrate that one single synoptic tracer test should not be directly generalized or interpreted without considering temporal dynamics and groundwater conditions.

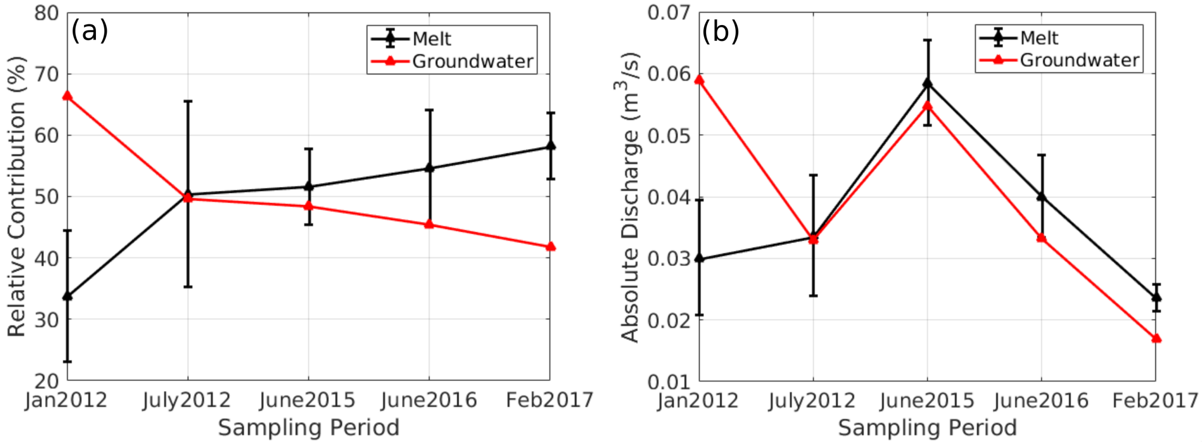

Figure 3. The HBCM mixing model predicts a range in relative meltwater contributions to discharge, which may reflect both temporal changes and uncertainties. Error bars bracket HBCM estimates that produced similar best matches to observed tracer concentrations; however, actual uncertainty are much higher because of the residual errors. Absolute meltwater discharge contributions can vary in time very differently than relative inputs, in part due to varying groundwater contributions.

Across all sampling periods, the groundwater fraction in the Gavilan Machay discharge appears high. When compared to an exponential fit between relative groundwater contribution and glacierized fraction for four watersheds in the Cordillera Blanca (Baraer et al., 2015), our HBCM-derived estimates are approximately twice as large. Furthermore, previous studies in the Cordillera Blanca found greater specific discharge in more highly glacierized areas (Baraer et al., 2009; Mark and Seltzer, 2003). In contrast, when we extended our HBCM analysis downgradient to the Boca Toma diversion point, results suggest that the glacierized Gavilan Machay sub-catchment has a specific discharge that is less than half of that in the non-glaciated portion of the Upper Río Mocha watershed. Wetter inner tropics climate and volcanic subsurface properties likely contribute to the distinct findings on Volcán Chimborazo.

HBCM implementation with five different field campaigns enabled us to evaluate uncertainties due to distinct sampling plans (details in Supplementary Information - Table S1). We found that changing HBCM cell configurations could generate up to a 23% melt fraction difference in estimates. Also, having fewer HBCM analysis cells (e.g., longer stream reaches) and fewer groundwater samples consistently led to greater HBCM residual errors. Too few groundwater samples becomes problematic when groundwater is not a homogeneous end-member throughout the watershed, which can be seen to be the case in Gavilan Machay from Figure 2(c), which shows spring samples containing higher solute concentrations at lower elevations. Further, groundwater end-member errors grow when using fewer and longer reach cells, while with additional and shorter reach cells, observations can reset the stream channel chemistry to correct concentrations. These results demonstrate the importance of adequately measuring the spatial variability of the surface and subsurface flow network, and they prompt the use of alternative methods to help constrain uncertainties in HBCM analysis results.

4.2 Time series analysis of hydroclimatic controls

Because of the uncertainties and long time gaps in the HBCM analyses, we applied time series analysis to the continuous data available from July 2015 to March 2016 at the Boca Toma weather station and Gavilan Machay gauging station to further infer characteristic trends between glacial melt and discharge and their climatic controls. Considering air temperature as a proxy indicator of glacial meltwater, the hourly cross correlation of air temperature leading discharge at Gavilan Machay in Figure 4(a) shows a strong diurnal signal, with peak discharge occurring four hours after the warmest part of the day at an average rate (0.1 m^3/s) that is about twice the magnitude of average morning discharge.

To determine if melt could be driving discharge variability beyond diurnal time scales, we examined the spectral squared coherence between temperature and discharge in Figure 4(c), which quantifies their correlation at a certain time frequencies (or periods). As expected from the time-series results, the most prominent feature is the peak at a period of 24 hours. Interestingly, the next highest coherence is at a period of 12 hours. While this could be a harmonic artifact of the dominant 24-hour trend, it is supported by a slight temperature increase commonly observed around 11pm, possibly due to adiabatic warming as downslope winds develop. The resulting increase in discharge, while detectable, is inconsequential to the total daily water balance. Other very narrow coherence peaks at periods less than 12 hours are likely spurious, because the power spectral densities of both temperature and discharge are low over that range (Figure S9). However, the smaller but broader peak around 50 to 60 hours

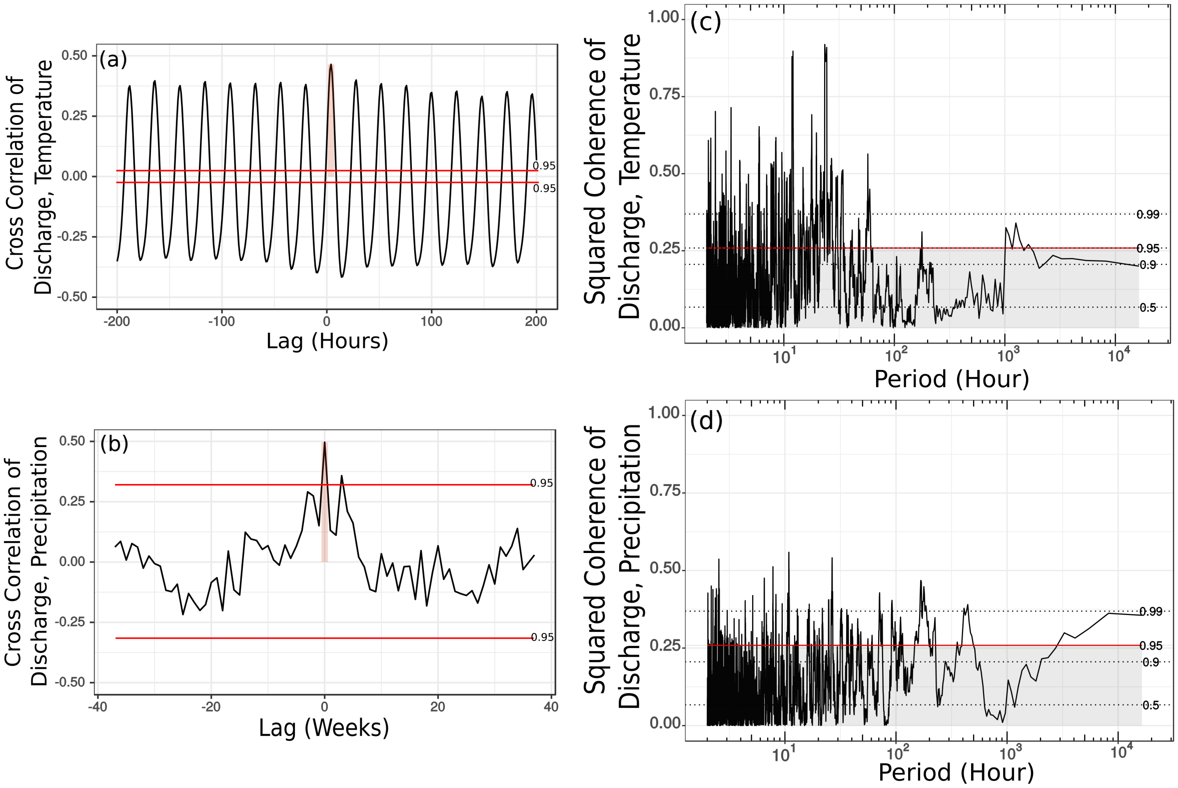

Figure 4. Cross-correlations (with 95% confidence interval shown) of observed discharge at Gavilan Machay with **(a)** hourly temperature and **(b)** weekly precipitation show that discharge has a clear diurnal link with temperature at about a 4 hour lag and a strong relationship with weekly precipitation, respectively. Spectral coherence (with various confidence intervals shown) between discharge and **(c)** temperature exhibits a high peak at 24 hours corresponding the cross-correlation result, as well as a strong peak at 12 hours, and more moderate peaks at multi-day scales. The coherence between discharge and **(d)** precipitation peaks between 100 to 200 hours (about 1 week) and may also be significant at scales approaching one year.

suggests that multi-day warming may also drive multi-day discharge events, though this link is much weaker than the diurnal response.

The substantial groundwater contributions to discharge inferred from the HBCM analysis prompts a look at not only melt but also precipitation controls on multi-day discharge. Hourly precipitation and discharge are very weakly correlated (Figure S10(a)); however, a correlation of r_{xy} =0.5 appears for weekly averages with zero time lag (Figure 4(b)). Correspondingly, a high (above 95% confidence interval) and broad coherence peak between precipitation and discharge can be seen over periods of about one week (168 hours). Together, these results suggest that sustained rain events influence discharge over a week, and therefore that rainwater tends to infiltrate instead of flow quickly overland. Other statistically significant (at the 95%

confidence interval) coherences between discharge and both temperature and precipitation across multi-week to multi-month periods further support slow subsurface flow pathways.

Combining the time series analysis with the HBCM results suggests that streamflow at Gavilan Machay is heavily influenced by both surficial meltwater and groundwater, and that the latter is driven by precipitation. Furthermore, time series and spectral analyses highlight temporal links not easily found through a fieldwork-intensive tracer-based approach: meltwater feeds discharge at Gavilan Machay on an hourly time scale, while weekly discharge responds most strongly to precipitation events. There are, however limitations to this statistical assessment that result from the short nine-month dataset, which precludes robust examination of any seasonal to multi-year responses to bimodal wet and dry seasons and El Niño effects. Hydrologic modeling in the following section can address this, as well as questions about detailed physical processes, such as quantifying how much melt contributions or groundwater may buffer periods of low rainfall.

4.3 Integrated Hydrologic Model Simulations

4.3.1 Calibration Results

Matching the observed discharge dynamics with the hydrologic model required calibration of two different melt factors based on time period: a lower value of 7.10 mm.w.e. (millimeters water equivalent) C^{-1} day^{-1} over December 2015-February 2016 and a higher value of 8.64 mm.we.$^{\circ}C^{-1}$ day^{-1} over the rest of the simulation. Our simulation period coincides with a strong El Niño event that generated the warmest and driest conditions from late November 2015 to the start of February 2016 (Figure 5(a)–(b)). The lower melt factor at this time dampens the intensity of melt, possibly because of the absence of heat transfer from rain (Francou, 2004), but it nonetheless simulates among the highest melt volumes of the simulation period (Figure 5(a)), consistent with other studies showing increased melt in response to El Niño events in the Andes (Francou, 2004; Veettil et al., 2014a; Manciati et al., 2014; Maussion et al., 2015; Veettil et al., 2016). Huss et al. (2009) similarly estimated a lower melt factor in the Swiss Alps when air temperature was high in response to longwave radiation. Overall, in Gavilan Machay, the average specific melt rate (in water equivalence) simulated over glaciated areas below the ELA was 1.5 m/yr. This falls within the range measured at the Reschreiter Glacier tongue, bracketed by geodetic mass balance estimates on slower-melting debris-covered ice of 0.87 m/yr (1997–2013) and 0.54 m/yr (June 2012–January 2013), and ablation stake observations on faster-melting clean ice of 3.4 m/yr (June–November 2016).

The calibration procedure also involved soil parameter adjustments. Hydraulic parameter estimates in páramo environments are scarce, and their characterization can be uncertain (Buytaert et al., 2006). For an initial estimate, we applied pedotransfer functions used in Flux-PIHM (Wosten et al., 1999) to a range of páramo soil measurements from a study area 20 km northwest of Chimborazo (3800 to 4200 m.a.s.l.) (Podwojewski et al., 2002) and from a study watershed on glaciated Volcán Antisana also in the Ecuadorian Andes (4000-4600 m.a.s.l.) (Minaya, 2016) (see supplementary information – Table S2 – for full details. We then calibrated the model for three mapped land-cover zones corresponding to páramo, rock/dirt/gravel, and ice (Figure 1). In the páramo zone (Table 1), matching observed discharge required lower hydraulic conductivity and greater water retention (expressed in van Genuchten hydraulic parameters) than initially estimated. This is likely due to high organic matter content

Hydrol. Earth Syst. Sci. Discuss., https://doi.org/10.5194/hess-2018-260
Manuscript under review for journal Hydrol. Earth Syst. Sci.
Discussion started: 31 May 2018

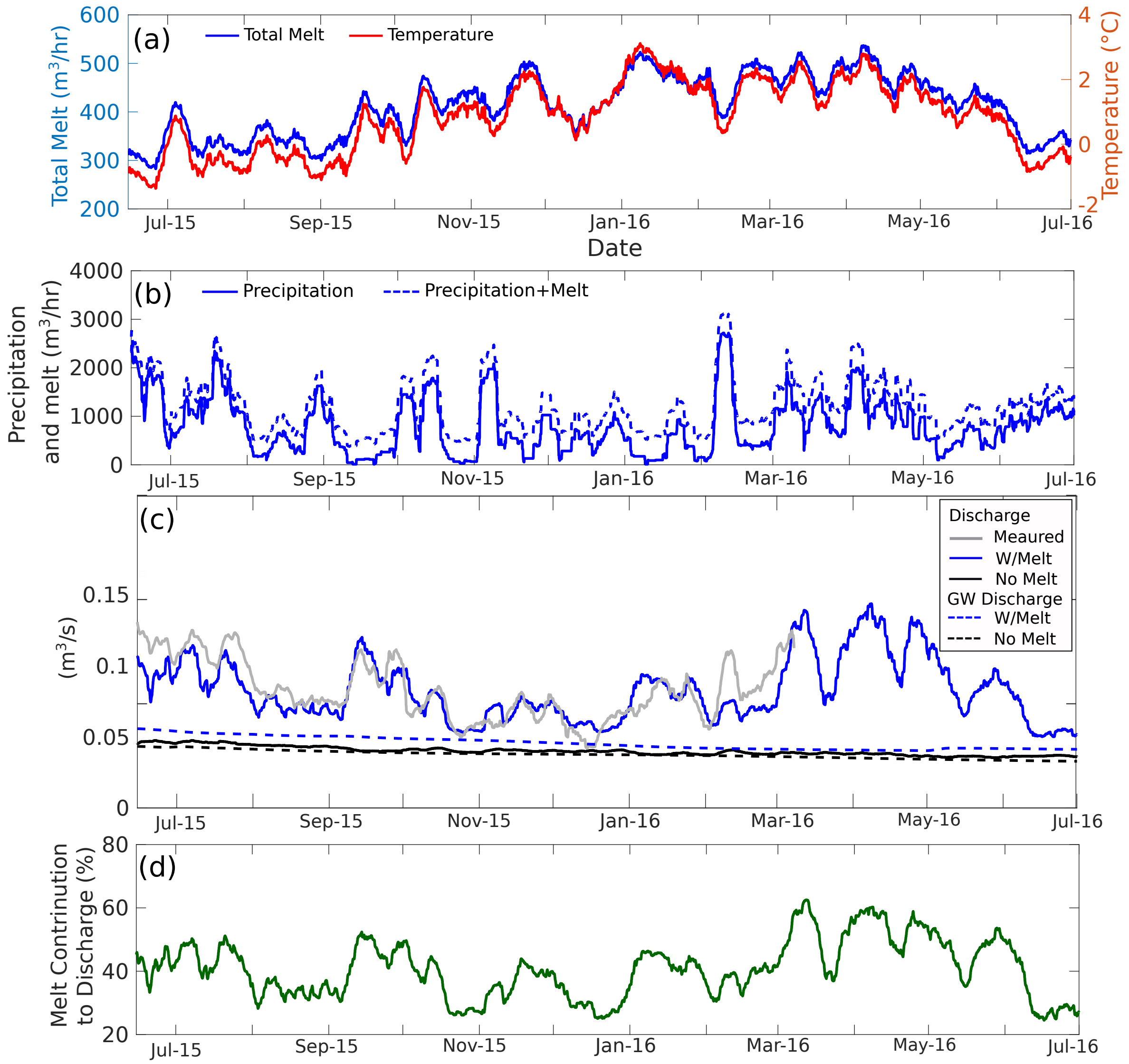

Figure 5. Time series of weekly moving average of **(a)** average air temperature below ELA (5050 m.a.s.l.) and over glaciers and simulated melt inputs; **(b)** precipitation (solid line), and precipitation+melt (dashed lines)) inputs **(c)** discharge at Gavilan Machay from observations (gray), calibrated simulations (blue solid), and simulations with no ice-melt (black solid); groundwater distribution to discharge for calibrated (blue dashed) and for no-ice simulations (black dashed); and **(d)** simulated percent melt contribution to discharge at Gavilan Machay.

supported by the study area's sub-humid conditions and the well-recognized retentive hydraulic properties of páramo soils (Podwojewski et al., 2002; Buytaert et al., 2006). In the sparsely vegetated and ice-covered zones, the calibration yielded higher hydraulic conductivities and lower water retentions than in the páramo zone, corresponding to reduced organic matter fraction

	KINF (m/s)	KSATV (m/s)	KSATH (m/s)	Porosity	Residual Moisture	α (1/m)	β (-)
Range predicted for observed páramo soil textures*	3.71E-8–8.28E-5	8.42E-8– 3.71E-5	8.42E-7– 6.96E-5	0.418– 0.493	0.05	0.327–5.82	1.1–1.173
Calibrated: Grassland$^\diamond$	1.23E-07	4.02E-08	4.02E-07	0.458	0.05	0.488	1.066
Calibrated: Sparsely vegetated$^\diamond$	1.43E-07	4.63E-08	4.63E-07	0.459	0.05	0.585	1.063
Calibrated: Ice-covered$^\diamond$	2.07E-07	6.71E-08	6.71E-07	0.461	0.05	0.863	1.06

*Predicted using pedotransfer functions with 9 páramo soil texture measurements from Ecuador. Samples are from 3 locations in a glaciated watershed in Volcan Antisana (Minaya, 2016) and 4 locations about 20 km northwest of Chimborazo (Podwojewski et al., 2002) (see Supplementary Information for more details).

$^\diamond$Calibrated to match observed discharge at Gavilan Machay

Table 1. Soil hydraulic parameters calibrated for the three soil type areas compared against the range predicted using the pedotransfer function with measured páramo soil textures in Ecuador (Podwojewski et al., 2002; Minaya, 2016). Parameters include hydraulic conductivities for vertical infiltration (KINFV), vertical unsaturated zone flow (KSATV), and horizontal saturated zone flow (KSATH); porosity (SMCMAX); residual soil moisture (SMCMIN); and shape parameters (α and β) for the van Genuchten moisture retention curve: $\theta = \theta_{res} + porosity \times (\frac{1}{1+abs(\alpha \times \psi)})^{\beta}))^{(1-\frac{1}{\beta})}$, with pressure head ψ.

and fractured bedrock, though the hydraulic conductivities were still lower than the initial estimates from the pedotransfer functions.

Simulation results in Figure 5(c) show that the calibrated model parameters closely produced the observed weekly discharge, including lower discharge under the drier and warmer El Niño conditions in December 2015-January 2016. The single major model mismatch occurred at a precipitation-driven discharge peak in February 2016. This could reflect uncertainties from the soil parameter calibration, as well as from our use of a lapse rate-based precipitation field over complex terrain, in which high-altitude precipitation events may not all be recorded at the low-altitude rain gauge. On shorter timescales, hour-of-day simulation results in Figure 6(b) demonstrate that the model does produce a diurnal trend, but with slightly less than half the average range and at a 6-hour later peak compared to observations (Figure 6(a)). These hourly discrepancies can be attributed to weaknesses in the simple melt model. Hock (2005) argued that TI models can successfully capture seasonal glacier melt trends but struggle with diurnal fluctuations, which are strongly driven by solar radiation dynamics. Although our simulations cannot reliably produce the timing of hourly discharge, they can provide informative lower bounds on the average diurnal range.

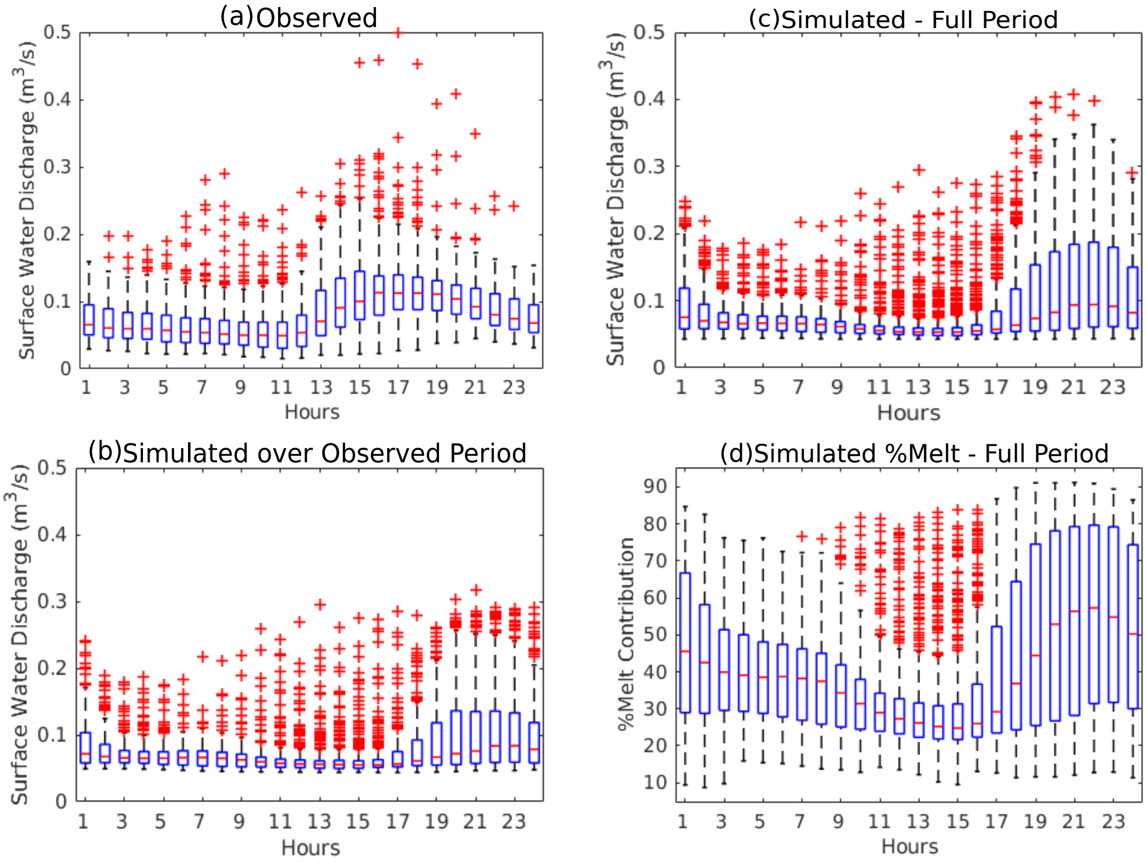

Figure 6. Box plots over local hour-of-day showing 25 – 75 percentiles with boxes and maximum and minimum with whiskers for **(a)** observed discharge over the 9-month observation period, **(b)** simulated discharge over the 9-month observation period, **(c)** simulated discharge over the 12-month simulation period, and **(d)** simulated percent melt contribution to discharge over the 12-month period. Simulations do capture diurnal patterns, but with an underestimated magnitude and shifted peak. Simulated percent melt contributions to discharge closely mirror the simulated diurnal fluctuations in discharge.

4.3.2 Simulations of relative melt contribution to discharge

To quantify relative glacial meltwater contribution to stream discharge using Flux-PIHM, we compared the calibrated discharge simulations at Gavilan Machay (Q_{Calib}) with simulations that omitted meltwater in the forcing inputs (Q_{NoMelt}). We then calculated relative glacial meltwater contribution to discharge via:

5 $$\%Melt = \frac{Q_{Calib} - Q_{NoMelt}}{Q_{Calib}} \times 100\%. \quad (2)$$

This estimate represents the additional discharge due to glacier melt, but may not exactly correspond to HBCM results for a number of reasons. First, the water balance impact of glacier melt conveyed in equation (2) may not equal the proportion of meltwater in a sample of discharge water if, for example, melt inputs facilitate more runoff of precipitation-sourced water. Also, while equation (2) isolates just the effect of glacier melt, HBCM estimates could include snow-melt, depending on the composition of the meltwater sample taken just below the glacier tongue. Lastly, any melt that infiltrates is considered as part of the groundwater rather than melt fraction in HBCM estimates, while equation (2) includes the effect of both surficial and groundwater contributions of meltwater to discharge.

These conceptual discrepancies complicate comparisons between the two methods, but it is possible to assess the June 20-25, 2016 HBCM result against the simulation (other HBCM periods fall outside the one-year model period). During June 20-25, 2016, the 45-64% estimate with HBCM is higher than the average simulated relative melt contribution of 29%, but it falls within the simulated hourly range of 13-70% over that time. Considering that samples were collected during the daytime when melt contributions were generally high, the results from these two approaches reasonably agree.

While process-driven temporal patterns were difficult to glean from the sparsely spaced and uncertain HBCM results, Flux-PIHM simulations in Figure 5(d) clearly indicate considerable variability in weekly melt contributions of 25–61% over June 2015–June 2016. This range compares very closely with the 23–66% range bounded by the five HBCM estimates spanning January 2012 to February 2017, lending further confidence in the consistency between the watershed and mixing model results, despite the differences in temporal and other types of representation noted above. Hourly distributions of simulated melt contribution in Figure 6(d) show an average diurnal range of 25-68%; given that the actual range is likely even broader due to underestimations by the temperature index model, diurnal fluctuations in relative melt contributions may be of similar or even greater magnitude than changes on weekly to monthly timescales.

Comparing Figures 5(c) and (d) reveals a remarkably strong correlation (0.89) between simulated weekly discharge and relative melt contributions, indicating that major discharge peaks over multi-day timescales are melt-driven, a link that was masked in the time series analysis in Section 4.2 by the overwhelming diurnal signal between temperature and discharge. Figure 7(a) shows strong coherence over 30 to 80 day periods between simulated melt inputs and relative melt contributions to discharge, highlighting those timescales as the most prominent beyond diurnal correlations. Most (86%) of the melt contribution to discharge occurred through surface runoff processes in the model, consistent with the hourly correlations found between observed discharge and temperature in Section 4.2. With the model, the influence of melt on discharge is clear during times such as early January 2016, when an uptick in discharge occurs despite low precipitation, due to warm temperatures and greater melt contribution (Figure 5).

Interestingly, the peak relative melt contributions (Figure 5(d)) do not always align with melt production patterns (Figure 5(a)) (e.g., in early February 2017, percent melt contribution peaks just when temperature and melt inputs dip), and their weekly correlation is not strong at a 95% confidence level (Figure S10(b)). Squared coherences in Figure 7(a) indicate that this is because relative melt contribution also responds to precipitation inputs, and this happens at weekly and multi-month timescales when correlations with melt inputs are low (Figure 7(b)). In fact, the strong coherence between precipitation and melt contribution around 6 to 14 day periods reveals that the high correlation between observed weekly precipitation and discharge

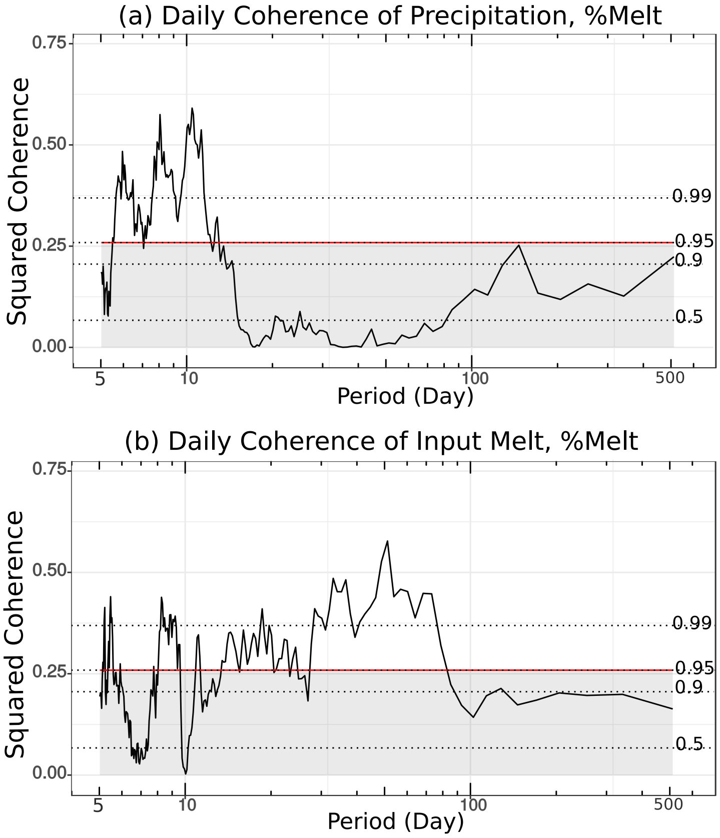

Figure 7. Coherences between simulated percent melt contribution to discharge with **(a)** precipitation and **(b)** simulated melt input. Calculations used daily average data to avoid known uncertainties in modeling diurnal fluctuations. Precipitation and melt inputs appear to be related to melt contributions at complementary timescales.

in Section 4.3 relates to melt contributions. Inspection of time periods such as mid-February and the start of April 2016 (Figure 5) show that rainy periods can augment melt inputs. During those times, increases in relative melt contributions to discharge coincided with precipitation events during local drops in melt input (Figure 5), possibly because weeklong precipitation creates antecedent moisture conditions that enhance the fraction of meltwater that runs off over the surface. Surface runoff can be expected to contain mostly meltwater or high-elevation precipitation, because runoff generally does not occur on low-elevation páramo soils except under intense precipitation (Sarmiento, 2000; Harden, 2004).

At greater timescales, significant coherences between precipitation and simulated relative melt contributions around 120+ days (Figure 7) correspond to overall lowest relative melt contributions during the dry El Niño period (December 2015-February 2016) and highest relative contributions during the two wet seasons (February-May and October-November). These melt contribution responses to bi-seasonal to interannual climatic patterns likely occur through slower groundwater pathways; the simulation with melt produces 18% greater groundwater contributions to discharge than that without melt (Figure 5(c)).

This supports the hypothesis that some amount of meltwater infiltrates and recharges to groundwater that then discharges farther downgradient to the stream channel. It should be noted, however, that the subsurface component of Flux-PIHM contains only a single shallow saturated zone, which mostly closely corresponds to a perched water table in the soil zone. This model implementation may not accurately represent additional deeper fractured bedrock aquifers systems, which could discharge groundwater to streams over shorter, multi-month time scales (Andermann et al., 2012), in contrast to the relatively constant groundwater dynamics simulated in Figure 5(c).

Our results may be particular to the more moist climate in the Gavilan Machay watershed, which supports constant groundwater discharge to the stream throughout the year and reflects compounded effects of melt inputs and rainfall conditions. However, although melt intensifies discharge variability in this watershed, a baseline 25% melt contribution throughout the simulation period indicates that a constant minimum level of melt helps prevent episodes of even more extreme low flows during drought times, such as during El Niño conditions. Overall, an average 52% of discharge can be attributed to melt inputs over the model simulation test period.

5 Summary and Conclusions

Although meltwater is typically credited with modulating stream discharge by buffering periods of low precipitation, we demonstrate using a combination of methods that relative meltwater contributions may drive nearly all the variability in discharge (correlation of 0.89) over a range of hourly to multi-year timescales in a humid glacierized watershed in the Ecuadorian Andes. Hydrochemical mixing model results for five sampling periods spanning 2012-2017 showed the meltwater fraction in discharge may have varied over approximately 20–65%. Hydrologic model simulations over June 2015–June 2016 produced a nearly identical range for weekly contributions. The model also predicted a very similar average diurnal range, which likely provided a lower bound of actual variability based on hydroclimatic data. This multi-scale variability in melt contributions can be attributed to dynamic climate forcings that also contain a range of temporal patterns (Figure 8). We found a strong correlation between diurnal temperature and discharge changes that likely reflects melt inputs and supports the use of a temperature index melt model (Figure 8(a)). Although such a simple melt approach somewhat underestimated hourly fluctuation extremes with a lag, it led to reasonable weekly discharge predictions when implemented with a seasonally variable melt factor that possibly accounts for additional heat transfer from rainfall during wet seasons. The hydrologic model showed that not only were diurnal discharge patterns responding to radiation-driven melt inputs, but relative melt contribution and discharge variations over 30-80 day periods were also controlled by melt inputs (Figure 8(c)).

Unexpectedly, model results showed that precipitation also boosted melt contributions to discharge, but on weekly and semi-annual timescales that complement the hourly and monthly timescales controlled by temperature and melt inputs. Weekly precipitation events likely generate antecedent wet conditions that facilitate greater amounts of meltwater runoff (Figure 8(b)), while longer-term precipitation patterns appear to drive slow changes in melt additions to groundwater (Figure 8(d)). Most (86%) melt contributions to discharge occurred through surface runoff in the model, but some meltwater recharged to groundwater, supporting a relatively steady groundwater discharge to the stream that is about 18% greater than in the scenario without

Hydrol. Earth Syst. Sci. Discuss., https://doi.org/10.5194/hess-2018-260
Manuscript under review for journal Hydrol. Earth Syst. Sci.
Discussion started: 31 May 2018

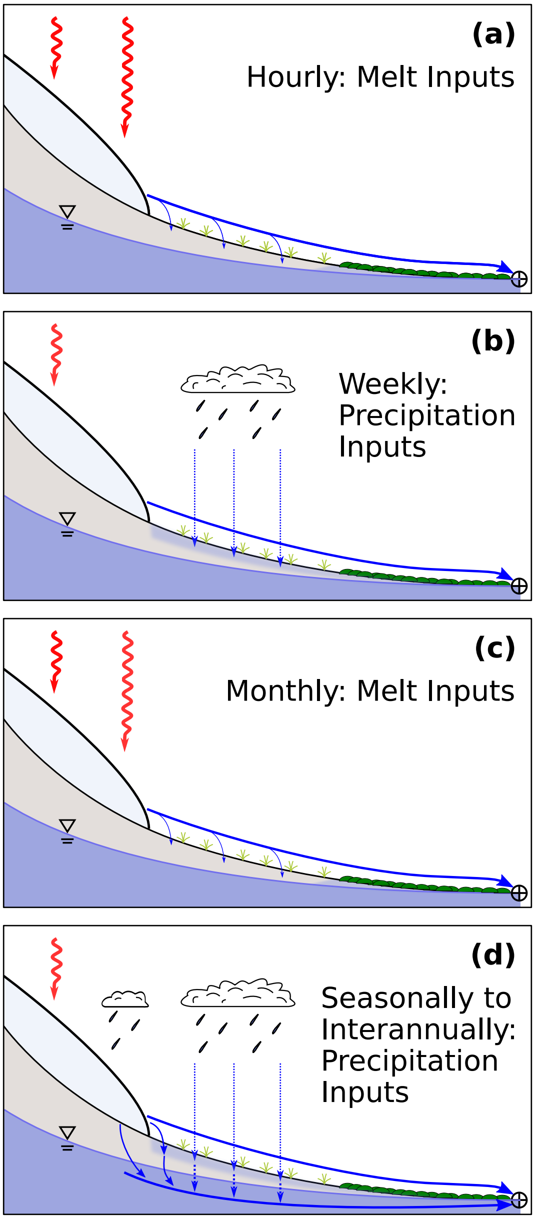

Figure 8. Relative melt contributions drive nearly all the variability in discharge in Gavilan Machay, mostly through surface runoff of glacial meltwater. What drives the variability in relative melt contributions to discharge? Our results show that this depends on the timescale. **(a)** Hourly timescale variability is controlled by radiation-driven (red arrows) melt inputs at the glacier tongue (light blue slab at upper left), which readily runs off overland (thick blue arrow) and eventually reaches the watershed's discharge point (circle with cross). **(b)** Weekly timescale variability is controlled by weekly precipitation events, which likely generate antecedent moisture conditions (light blue shading) that promote greater meltwater runoff. **(c)** Monthly timescale variability is driven by monthly trends in melt generation, which contributes to discharge mostly through surface runoff. **(d)** Seasonal to interannual variability is driven by long-term precipitation, which can enhance melt by transferring heat from rain (blue arrows right of glacier tongue), and augment subsurface melt contributions through increased groundwater flow (thick blue arrow below water table).

melt. As expected, strong El Niño conditions corresponded to some of the highest simulated melt inputs, but less easy to predict was that Gavilan Machay exhibited its lowest discharge during this time. Melt prevented streamflow from dropping below a baseline level during the warm and dry El Niño event, but discharge was much higher during wetter periods, in part because of the rainfall-enhanced melt contributions described above.

The multiscale temporal variability of relative melt contributions to discharge has important implications for how to determine the hydrologic role of glaciers in watersheds, as well as for water resource management in fast-changing glacierized systems. Care must be taken in the implementation and interpretation of commonly employed tracer analyses. Potentially large diurnal fluctuations make it imperative to collect samples over consistent times of day, and weekly to interannual variability complicate extrapolations from single synoptic sampling estimates. Recharge of meltwater further confounds the interpretation of groundwater as a source entirely distinct from surficial meltwater. These uncertainties, along with additional errors caused by heterogeneous groundwater chemistry and the choice of sample locations, limit the ability of tracer-based analyses to constrain dynamic melt contributions to discharge. Model simulations provide ideal temporal resolution, but they suffer from their own disadvantages. Easy to implement temperature-index models may not be reliable for predicting the full magnitude and timing of diurnal melt pulses, and they may require seasonal calibration of melt factors. Difficulties in obtaining soil and vegetation properties lead to further model errors.

For water resources, weekly to multi-year melt contributions to discharge are of greater interest than hourly fluctuations. At those timescales of concern, rain events and wet periods can accentuate relative melt contributions to streamflow in humid glacierized systems. This signifies a bonus in water yield, but it also intensifies discharge variability over weekly and seasonal timescales, which can pose challenges if water storage infrastructure is unavailable. On an interannual basis, melt can augment discharge during warm and dry El Niño events, but glacierized watersheds will likely experience greatest melt contributions during wetter times, when they are under the combined effects of enhanced ablation and precipitation. In the future, should Reschreiter Glacier melt completely, overall discharge in Gavilan Machay could decrease by more than 50%, even if precipitation remains adequate to maintain a relatively constant groundwater flow. This suggests that in response to glacier loss in a warming climate, glacierized watersheds in the humid inner tropics may eventually experience steadier discharge, but at significantly decreased rates.

Code and data availability. The version of Flux-PIHM used for this paper is available on GitHub, at https://github.com/PSUmodeling/MM-PIHM. The PIHMgis software used to create input files is available at http://www.pihm.psu.edu/pihmgis_downloads.html. The corresponding author may be contacted to access field data collected and used in this work.

Author contributions. Saberi implemented the time series analysis and hydrologic modeling, assisted with the mixing model analysis, and contributed to writing the manuscript. McLaughlin executed the field work in 2016-2017, implemented the mixing model analysis, and contributed to writing the manuscript. Ng conceived of the project together with La Frenierre, oversaw the analysis, and contributed to

writing the manuscript. La Frenierre also established the study site and led the fieldwork. Wickert provided field instrumentation for 2015-2017 and contributed to fieldwork. Baraer provided the HBCM mixing model software and guided its implementation. Zhi and Li assisted with the Flux-PIHM hydrologic model implementation. Mark supported establishment of the field site and supervised initial work.

Competing interests. The authors declare that they have no conflict of interest.

Acknowledgements. McLaughlin received travel support from University of Minnesota's Walter H. Judd Fellowship. Ng and Wickert received financial support from University of Minnesota. La Frenierre received financial support from the National Science Foundation's Doctoral Dissertation Research Improvement Grant (#1103235); the Fulbright Commission of Ecuador, the Geological Society of America, and Gustavus Adolphus College. The authors would like to acknowledge field assistance from Chad Sandell, Casey Decker, Helen Thompson, and Abigail Michels; lab support from Jeff Jeremiason, Chris Harmes, and Scott Alexander; and land-cover mapping assistance from Josh Zoellmer.

References

Andermann, C., Longuevergne, L., Bonnet, S., Crave, A., Davy, P., and Gloaguen, R.: Impact of transient groundwater storage on the discharge of Himalayan rivers, Nature Geoscience, 5, 127–132, https://doi.org/10.1038/ngeo1356, 2012.

Andrews, E. D.: Measurement and computation of bed-material discharge in a shallow sand-bed stream, Muddy Creek, Wyoming, Water Resources Research, 17, 131–141, https://doi.org/10.1029/WR017i001p00131, 1981a.

Andrews, E. D.: Measurement and computation of bed-material discharge in a shallow sand-bed stream, Muddy Creek, Wyoming, Water Resources Research, 17, 131–141, https://doi.org/10.1029/WR017i001p00131, 1981b.

Baraer, M., McKenzie, J. M., Mark, B. G., Bury, J., and Knox, S.: Characterizing contributions of glacier melt and groundwater during the dry season in a poorly gauged catchment of the Cordillera Blanca (Peru), Advances in Geosciences, 22, 41–49, https://doi.org/10.5194/adgeo-22-41-2009, 2009.

Baraer, M., Mark, B. G., McKenzie, J. M., Condom, T., Bury, J., Huh, K.-I., Portocarrero, C., Gómez, J., and Rathay, S.: Glacier recession and water resources in Peru's Cordillera Blanca, Journal of Glaciology, 58, 134–150, https://doi.org/10.3189/2012JoG11J186, 2012.

Baraer, M., McKenzie, J., Mark, B. G., Gordon, R., Bury, J., Condom, T., Gomez, J., Knox, S., and Fortner, S. K.: Contribution of groundwater to the outflow from ungauged glacierized catchments: a multi-site study in the tropical Cordillera Blanca, Peru, Hydrological Processes, 29, 2561–2581, https://doi.org/10.1002/hyp.10386, 2015.

Barba, D., Samaniego, P., Eissen, J.-p., Robin, C., Fornari, M., Cotten, J., and Beate, B.: Geology and structure of the late Pleistocene to Holocene Chimborazo stratovolcano (Ecuador), 6th International Symposium on Andean Geodynamics (ISAG 2005, Barcelona), pp. 90–93, 2005.

Barnett, T. P., Adam, J. C., and Lettenmaier, D. P.: Potential impacts of a warming climate on water availability in snow-dominated regions, Nature, 438, 303–309, https://doi.org/10.1038/nature04141, 2005.

Bhatt, G., Kumar, M., and Duffy, C. J.: A tightly coupled GIS and distributed hydrologic modeling framework, Environmental Modelling & Software, 62, 70–84, https://doi.org/10.1016/j.envsoft.2014.08.003, 2014.

Bradley, R. S.: CLIMATE CHANGE: Threats to Water Supplies in the Tropical Andes, Science, 312, 1755–1756, https://doi.org/10.1126/science.1128087, 2006.

Bradley, R. S., Vuille, M., Hardy, D., and Thompson, L. G.: Low latitude ice cores record Pacific sea surface temperatures, Geophysical Research Letters, 30, 2–5, https://doi.org/10.1029/2002GL016546, 2003.

Braun, L. N., Weber, M., and Schulz, M.: Consequences of climate change for runoff from Alpine regions, Annals of Glaciology, 31, 19–25, https://doi.org/10.3189/172756400781820165, 2000.

Bury, J., Mark, B. G., Carey, M., Young, K. R., McKenzie, J. M., Baraer, M., French, A., and Polk, M. H.: New Geographies of Water and Climate Change in Peru: Coupled Natural and Social Transformations in the Santa River Watershed, Annals of the Association of American Geographers, 103, 363–374, https://doi.org/10.1080/00045608.2013.754665, 2013.

Bury, J. T., Mark, B. G., McKenzie, J. M., French, A., Baraer, M., Huh, K. I., Zapata Luyo, M. A., and Gómez López, R. J.: Glacier recession and human vulnerability in the Yanamarey watershed of the Cordillera Blanca, Peru, Climatic Change, 105, 179–206, https://doi.org/10.1007/s10584-010-9870-1, 2011.

Buytaert, W. and Beven, K.: Models as multiple working hypotheses: hydrological simulation of tropical alpine wetlands, Hydrological Processes, 25, 1784–1799, https://doi.org/10.1002/hyp.7936, 2011.

Buytaert, W., Célleri, R., De Bièvre, B., Cisneros, F., Wyseure, G., Deckers, J., and Hofstede, R.: Human impact on the hydrology of the Andean páramos, Earth-Science Reviews, 79, 53–72, https://doi.org/10.1016/j.earscirev.2006.06.002, 2006.

Caceres, B., Francou, B., Favier, V., Bontron, G., Tachker, P., Bucher, R., Taupin, J.-D., Vuille, M., Maisincho, L., and Delachaux, F.: Glacier 15, Antisana, Ecuador: its glaciology and relations to water resources, 2006.

Carey, M., Molden, O. C., Rasmussen, M. B., Jackson, M., Nolin, A. W., and Mark, B. G.: Impacts of Glacier Recession and Declining Meltwater on Mountain Societies, Annals of the American Association of Geographers, 107, 350–359, https://doi.org/10.1080/24694452.2016.1243039, 2017.

Cauvy-Fraunié, S., Condom, T., Rabatel, A., Villacis, M., Jacobsen, D., and Dangles, O.: Technical Note: Glacial influence in tropical mountain hydrosystems evidenced by the diurnal cycle in water levels, Hydrology and Earth System Sciences, 17, 4803–4816, https://doi.org/10.5194/hess-17-4803-2013, 2013.

Chen, J., Knight, R., and Zebker, H. A.: The Temporal and Spatial Variability of the Confined Aquifer Head and Storage Properties in the San Luis Valley, Colorado Inferred From Multiple InSAR Missions, Water Resources Research, 53, 9708–9720, https://doi.org/10.1002/2017WR020881, 2017.

Christophersen, N., Neal, C., Hooper, R. P., Vogt, R. D., and Andersen, S.: Modelling streamwater chemistry as a mixture of soilwater end-members—a step towards second-generation acidification models, Journal of Hydrology, 116, 307–320, 1990.

Clapperton, C. M.: Glacial and volcanic geomorphology of the Chimborazo-Carihuairazo Massif, Ecuadorian Andes, Transactions of the Royal Society of Edinburgh: Earth Sciences, 81, 91–116, https://doi.org/10.1017/S0263593300005174, 1990.

Clow, D., Schrott, L., Webb, R., Campbell, D., Torizzo, A., and Dornblaser, M.: Ground Water Occurrence and Contributions to Streamflow in an Alpine Catchment, Colorado Front Range, Ground Water, 41, 937–950, https://doi.org/10.1111/j.1745-6584.2003.tb02436.x, 2003.

Crossman, J., Bradley, C., Boomer, I., and Milner, A. M.: Water Flow Dynamics of Groundwater-Fed Streams and Their Ecological Significance in a Glacierized Catchment, Arctic, Antarctic, and Alpine Research, 43, 364–379, https://doi.org/10.1657/1938-4246-43.3.364, 2011.

Ek, M. B., Mitchell, K. E., Lin, Y., Rogers, E., Grunmann, P., Koren, V., Gayno, G., and Tarpley, J. D.: Implementation of Noah land surface model advances in the National Centers for Environmental Prediction operational mesoscale Eta model, Journal of Geophysical Research: Atmospheres, 108, 2003.

Engel, M., Penna, D., Bertoldi, G., Dell'Agnese, A., Soulsby, C., and Comiti, F.: Identifying run-off contributions during melt-induced run-off events in a glacierized alpine catchment, Hydrological Processes, 30, 343–364, https://doi.org/10.1002/hyp.10577, 2016.

Escher-Vetter, H., Reinwarth, O., and Rentsch, H.: Two decades of runoff measurements (1974 to 1993) at the pegelstation Vernagtbach/Oetztal alps, Zeitschrift für Gletscherkunde und Glazialgeologie, 30, 99–107, 1994.

Farr, T. G., Rosen, P. A., Caro, E., Crippen, R., Duren, R., Hensley, S., Kobrick, M., Paller, M., Rodriguez, E., and Roth, L.: The shuttle radar topography mission, Reviews of Geophysics, 45, 2007.

Favier, V.: Glaciers of the outer and inner tropics: A different behaviour but a common response to climatic forcing, Geophysical Research Letters, 31, L16 403, https://doi.org/10.1029/2004GL020654, 2004.

Favier, V., Coudrain, A., Cadier, E., Francou, B., Ayabaca, E., Maisincho, L., Praderio, E., Villacis, M., and Wagnon, P.: Evidence of groundwater flow on Antizana ice-covered volcano, Ecuador / Mise en évidence d'écoulements souterrains sur le volcan englacé Antizana, Equateur, Hydrological Sciences Journal, 53, 278–291, https://doi.org/10.1623/hysj.53.1.278, 2008a.

Favier, V., Coudrain, A., Cadier, E., Francou, B., Ayabaca, E., MAISINCHO, L., Praderio, E., Villacis, M., and Wagnon, P.: Evidence of groundwater flow on Antizana ice-covered volcano, Ecuador / Mise en évidence d'écoulements souterrains sur le volcan englacé Antizana, Equateur, Hydrological Sciences Journal, 53, 278–291, https://doi.org/10.1623/hysj.53.1.278, 2008b.

Fernández, A. and Mark, B. G.: Modeling modern glacier response to climate changes along the Andes Cordillera: A multiscale review, Journal of Advances in Modeling Earth Systems, 8, 467–495, 2016.

Fountain, A. G. and Tangborn, W. V.: The Effect of Glaciers on Streamflow Variations, Water Resources Research, 21, 579–586, https://doi.org/10.1029/WR021i004p00579, 1985.

Francou, B.: Tropical climate change recorded by a glacier in the central Andes during the last decades of the twentieth century: Chacaltaya, Bolivia, 16S, Journal of Geophysical Research, 108, 4154, https://doi.org/10.1029/2002JD002959, 2003.

Francou, B.: New evidence for an ENSO impact on low-latitude glaciers: Antizana 15, Andes of Ecuador, Journal of Geophysical Research, 109, D18 106, https://doi.org/10.1029/2003JD004484, 2004.

Frenierre, J. L. and Mark, B. G.: A review of methods for estimating the contribution of glacial meltwater to total watershed discharge, Progress in Physical Geography, 38, 173–200, https://doi.org/10.1177/0309133313516161, 2014.

Gabbi, J., Carenzo, M., Pellicciotti, F., Bauder, A., and Funk, M.: A comparison of empirical and physically based glacier surface melt models for long-term simulations of glacier response, Journal of Glaciology, 60, 1140–1154, https://doi.org/10.3189/2014JoG14J011, 2014.

Gordon, R. P., Lautz, L. K., McKenzie, J. M., Mark, B. G., Chavez, D., and Baraer, M.: Sources and pathways of stream generation in tropical proglacial valleys of the Cordillera Blanca, Peru, Journal of Hydrology, 522, 628–644, https://doi.org/10.1016/j.jhydrol.2015.01.013, 2015.

Harden, D. R.: California geology, Prentice Hall, 2004.

Harpold, A. A. and Brooks, P. D.: Humidity determines snowpack ablation under a warming climate, Proceedings of the National Academy of Sciences, 115, 1215–1220, https://doi.org/10.1073/pnas.1716789115, 2018.

He, Z., Vorogushyn, S., Unger-Shayesteh, K., Gafurov, A., Kalashnikova, O., Omorova, E., and Merz, B.: The value of hydrograph partitioning curves for calibrating hydrological models in glacierized basins, Water Resources Research, pp. 1–52, https://doi.org/10.1002/2017WR021966, 2018.

Hock, R.: A distributed temperature-index ice- and snowrnelt model including potential direct solar radiation, Journal qf Glaciology, 45, 1999.

Hock, R.: Glacier melt: a review of processes and their modelling, Progress in physical geography, 29, 362–391, 2005.

Hooper, R. P.: Diagnostic tools for mixing models of stream water chemistry, Water Resources Research, 39, 2003.

Hooper, R. P. and Shoemaker, C. A.: A Comparison of Chemical and Isotopic Hydrograph Separation, Water Resources Research, 22, 1444–1454, https://doi.org/10.1029/WR022i010p01444, 1986.

Huss, M., Bauder, A., Funk, M., and Hock, R.: Determination of the seasonal mass balance of four Alpine glaciers since 1865, Journal of Geophysical Research, 113, F01 015, https://doi.org/10.1029/2007JF000803, 2008.

Huss, M., Funk, M., and Ohmura, A.: Strong Alpine glacier melt in the 1940s due to enhanced solar radiation, Geophysical Research Letters, 36, L23 501, https://doi.org/10.1029/2009GL040789, 2009.

Immerzeel, W. W., van Beek, L. P. H., and Bierkens, M. F. P.: Climate Change Will Affect the Asian Water Towers, Science, 328, 1382–1385, https://doi.org/10.1126/science.1183188, 2010.

INEC: Cencos de Poblacion y Vivienda 2010, Quito, Ecuador, 2010.

James, A. L. and Roulet, N. T.: Investigating the applicability of end-member mixing analysis (EMMA) across scale: A study of eight small, nested catchments in a temperate forested watershed, Water Resources Research, 42, 2006.

Jansson, P., Hock, R., and Schneider, T.: The concept of glacier storage: a review, Journal of Hydrology, 282, 116–129, https://doi.org/10.1016/S0022-1694(03)00258-0, 2003.

Jasechko, S., Kirchner, J. W., Welker, J. M., and McDonnell, J. J.: Substantial proportion of global streamflow less than three months old, Nature Geoscience, 9, 126–129, https://doi.org/10.1038/ngeo2636, 2016.

Juen, I., Kaser, G., and Georges, C.: Modelling observed and future runoff from a glacierized tropical catchment (Cordillera Blanca, Perú), Global and Planetary Change, 59, 37–48, https://doi.org/10.1016/j.gloplacha.2006.11.038, 2007.

Kaser, G.: A review of the modern fluctuations of tropical glaciers, Global and Planetary Change, 22, 93–103, https://doi.org/10.1016/S0921-8181(99)00028-4, 1999.

Kaser, G. and Osmaston, H.: Tropical glaciers, Cambridge University Press, 2002.

Kendall, C., Doctor, D., Drever, J., Holland, H., and Turekian, K.: Stable isotope applications in hydrological studies, pp. 319–364, https://doi.org/http://dx.doi.org/10.1016/B0-08-043751-6/05081-7, 2003.

La Frenierre, J. and Mark, B. G.: Detecting Patterns of Climate Change at Volcán Chimborazo, Ecuador, by Integrating Instrumental Data, Public Observations, and Glacier Change Analysis, Annals of the American Association of Geographers, 107, 979–997, https://doi.org/10.1080/24694452.2016.1270185, 2017.

Lang, H.: Forecasting Meltwater Runoff from Snow-Covered Areas and from Glacier Basins, pp. 99–127, Springer Netherlands, Dordrecht, https://doi.org/10.1007/978-94-009-4536-4_5, 1986.

Liu, F., Williams, M. W., and Caine, N.: Source waters and flow paths in an alpine catchment, Colorado Front Range, United States, Water Resources Research, 40, 1–16, https://doi.org/10.1029/2004WR003076, 2004.

Lowry, C. S., Deems, J. S., Loheide II, S. P., and Lundquist, J. D.: Linking snowmelt-derived fluxes and groundwater flow in a high elevation meadow system, Sierra Nevada Mountains, California, Hydrological Processes, 24, 2821–2833, https://doi.org/10.1002/hyp.7714, 2010.

Lowry, C. S., Loheide, S. P., Moore, C. E., and Lundquist, J. D.: Groundwater controls on vegetation composition and patterning in mountain meadows, Water Resources Research, 47, 1–16, https://doi.org/10.1029/2010WR010086, 2011.

Luce, C. H.: Effects of Climate Change on Snowpack, Glaciers, and Water Resources in the Northern Rockies, pp. 25–36, Springer International Publishing, Cham, https://doi.org/10.1007/978-3-319-56928-4_3, 2018.

Mackay, A.: Climate Change 2007: Impacts, Adaptation and Vulnerability. Contribution of Working Group II to the Fourth Assessment Report of the Intergovernmental Panel on Climate Change, Journal of Environment Quality, 37, 2407, https://doi.org/10.2134/jeq2008.0015br, 2008.

Manciati, C., Villacís, M., Taupin, J.-D., Cadier, E., Galárraga-Sánchez, R., and Cáceres, B.: Empirical mass balance modelling of South American tropical glaciers: case study of Antisana volcano, Ecuador, Hydrological Sciences Journal, 59, 1519–1535, https://doi.org/10.1080/02626667.2014.888490, 2014.

Mark, B. G.: Tracing tropical Andean glaciers over space and time: Some lessons and transdisciplinary implications, Global and Planetary Change, 60, 101–114, https://doi.org/10.1016/j.gloplacha.2006.07.032, 2008.

Mark, B. G. and Mckenzie, J. M.: Tracing Increasing Tropical Andean Glacier Melt with Stable Isotopes in Water, Environmental Science & Technology, 41, 6955–6960, https://doi.org/10.1021/es071099d, 2007.

Mark, B. G. and Seltzer, G. O.: Tropical glacier meltwater contribution to stream discharge: a case study in the Cordillera Blanca, Peru, Journal of Glaciology, 49, 271–281, https://doi.org/10.3189/172756503781830746, 2003.

Mark, B. G., McKenzie, J. M., and Gómez, J.: Hydrochemical evaluation of changing glacier meltwater contribution to stream discharge: Callejon de Huaylas, Peru / Evaluation hydrochimique de la contribution évolutive de la fonte glaciaire à l'écoulement fluvial: Callejon de Huaylas, Pérou, Hydrological Sciences Journal, 50, 975–988, https://doi.org/10.1623/hysj.2005.50.6.975, 2005.

Markovich, K. H., Maxwell, R. M., and Fogg, G. E.: Hydrogeological response to climate change in alpine hillslopes, Hydrological Processes, 30, 3126–3138, https://doi.org/10.1002/hyp.10851, 2016.

Maussion, F., Gurgiser, W., Großhauser, M., Kaser, G., and Marzeion, B.: ENSO influence on surface energy and mass balance at Shallap Glacier, Cordillera Blanca, Peru, The Cryosphere, 9, 1663–1683, 2015.

McLaughlin, R.: Hydrochemical Signatures of Glacial Meltwater on Volcán Chimborazo, Ecuador, Ph.D. thesis, 2017.

Messerli, B., Viviroli, D., and Weingartner, R.: Mountains of the World: Vulnerable Water Towers for the 21st Century, AMBIO Special Report, 13, 29–34, https://doi.org/10.5167/uzh-110516, 2004.

Minaya, Maldonado, V. G.: Ecohydrology of the Andes Páramo Region, PhD diss., IHE Delft Institute for Water Education, 2016.

Ng, G.-H. C., Wickert, A. D., Somers, L. D., Saberi, L., Cronkite-Ratcliff, C., Niswonger, R. G., and McKenzie, J. M.: GSFLOW-GRASS v1. 0.0: GIS-enabled hydrologic modeling of coupled groundwater–surface-water systems, Manuscript under review for journal Geosci. Model Dev., 2018.

NRCS, U.: Part 630 Hydrology National Engineering Handbook, 2009.

Omani, N., Srinivasan, R., Smith, P. K., and Karthikeyan, R.: Glacier mass balance simulation using SWAT distributed snow algorithm, Hydrological Sciences Journal, 62, 546–560, https://doi.org/10.1080/02626667.2016.1162907, 2017.

Ostheimer, G. J., Hadjivasiliou, H., Kloer, D. P., Barkan, A., and Matthews, B. W.: Structural Analysis of the Group II Intron Splicing Factor CRS2 Yields Insights into its Protein and RNA Interaction Surfaces, Journal of Molecular Biology, 345, 51–68, https://doi.org/10.1016/j.jmb.2004.10.032, 2005.

Pellicciotti, F., Brock, B., Strasser, U., Burlando, P., Funk, M., and Corripio, J.: An enhanced temperature-index glacier melt model including the shortwave radiation balance: development and testing for Haut Glacier d'Arolla, Switzerland, Journal of Glaciology, 51, 573–587, 2005.

Pepin, N., Bradley, R. S., Diaz, H. F., Baraer, M., Caceres, E. B., Forsythe, N., Fowler, H., Greenwood, G., Hashmi, M. Z., Liu, X. D., Miller, J. R., Ning, L., Ohmura, A., Palazzi, E., Rangwala, I., Schöner, W., Severskiy, I., Shahgedanova, M., Wang, M. B., Williamson, S. N., and Yang, D. Q.: Elevation-dependent warming in mountain regions of the world, Nature Climate Change, 5, 424–430, https://doi.org/10.1038/nclimate2563, 2015.

Podwojewski, P., Poulenard, J., Zambrana, T., and Hofstede, R.: Overgrazing effects on vegetation cover and properties of volcanic ash soil in the pàramo of Llangahua and al Esperanza (Tungurahua, Ecuador), Management, 18, 45–55, https://doi.org/10.1079/SUM2001100, 2002.

Polk, M. H., Young, K. R., Baraer, M., Mark, B. G., McKenzie, J. M., Bury, J., and Carey, M.: Exploring hydrologic connections between tropical mountain wetlands and glacier recession in Peru's Cordillera Blanca, Applied Geography, 78, 94–103, https://doi.org/10.1016/j.apgeog.2016.11.004, 2017.

Pribulick, C. E., Foster, L. M., Bearup, L. A., Navarre-Sitchler, A. K., Williams, K. H., Carroll, R. W., and Maxwell, R. M.: Contrasting the hydrologic response due to land cover and climate change in a mountain headwaters system, Ecohydrology, 9, 1431–1438, https://doi.org/10.1002/eco.1779, 2016.

Qu, Y. and Duffy, C. J.: A semidiscrete finite volume formulation for multiprocess watershed simulation, Water Resources Research, 43, 1–18, https://doi.org/10.1029/2006WR005752, 2007.

Rabatel, A., Francou, B., Soruco, A., Gomez, J., Cáceres, B., Ceballos, J. L., Basantes, R., Vuille, M., Sicart, J.-E., Huggel, C., Scheel, M., Lejeune, Y., Arnaud, Y., Collet, M., Condom, T., Consoli, G., Favier, V., Jomelli, V., Galarraga, R., Ginot, P., Maisincho, L., Mendoza, J., Ménégoz, M., Ramirez, E., Ribstein, P., Suarez, W., Villacis, M., and Wagnon, P.: Current state of glaciers in the tropical Andes: a multi-century perspective on glacier evolution and climate change, The Cryosphere, 7, 81–102, https://doi.org/10.5194/tc-7-81-2013, 2013.

Reveillet, M., Vincent, C., Six, D., and Rabatel, A.: Which empirical model is best suited to simulate glacier mass balances?, Journal of Glaciology, 63, 39–54, https://doi.org/10.1017/jog.2016.110, 2017.

Rodell, M., Houser, P. R., Jambor, U. E. A., Gottschalck, J., Mitchell, K., Meng, C. J., Arsenault, K., Cosgrove, B., Radakovich, J., and Bosilovich, M.: The global land data assimilation system, Bulletin of the American Meteorological Society, 85, 381–394, 2004.

Ryu, J.-S., Lee, K.-S., and Chang, H.-W.: Hydrochemistry and isotope geochemistry of Song Stream, a headwater tributary of the South Han River, South Korea, Geosciences Journal, 11, 157–164, https://doi.org/10.1007/BF02913929, 2007.

Samaniego, P., Barba, D., Robin, C., Fornari, M., and Bernard, B.: Eruptive history of Chimborazo volcano (Ecuador): A large, ice-capped and hazardous compound volcano in the Northern Andes, Journal of Volcanology and Geothermal Research, 221-222, 33–51, https://doi.org/10.1016/j.jvolgeores.2012.01.014, 2012.

Sarmiento, L.: Water Balance and Soil Loss under Long Fallow Agriculture in the Venezuelan Andes, Mountain Research and Development, 20, 246–253, 2000.

Schmieder, J., Garvelmann, J., Marke, T., and Strasser, U.: Spatio-temporal tracer variability in the glacier melt end-member - How does it affect hydrograph separation results?, Hydrological Processes, 2016, https://doi.org/10.1002/hyp.11628, 2018.

Shi, Y., Davis, K. J., Duffy, C. J., and Yu, X.: Development of a Coupled Land Surface Hydrologic Model and Evaluation at a Critical Zone Observatory, Journal of Hydrometeorology, 14, 1401–1420, https://doi.org/10.1175/JHM-D-12-0145.1, 2013.

Sicart, J. E., Hock, R., and Six, D.: Glacier melt, air temperature, and energy balance in different climates: The Bolivian Tropics, the French Alps, and northern Sweden, Journal of Geophysical Research, 113, D24 113, https://doi.org/10.1029/2008JD010406, 2008.

Smith, J. A., Mark, B. G., and Rodbell, D. T.: The timing and magnitude of mountain glaciation in the tropical Andes, Journal of Quaternary Science, 23, 609–634, https://doi.org/10.1002/jqs.1224, 2008.

Soruco, A., Vincent, C., Rabatel, A., Francou, B., Thibert, E., Sicart, J. E., and Condom, T.: Contribution of glacier runoff to water resources of La Paz city, Bolivia (16° S), Annals of Glaciology, 56, 147–154, https://doi.org/10.3189/2015AoG70A001, 2015.

Soulsby, C., Petry, J., Brewer, M., Dunn, S., Ott, B., and Malcolm, I.: Identifying and assessing uncertainty in hydrological pathways: a novel approach to end member mixing in a Scottish agricultural catchment, Journal of Hydrology, 274, 109–128, https://doi.org/10.1016/S0022-1694(02)00398-0, 2003.

Staudinger, M., Stoelzle, M., Seeger, S., Seibert, J., Weiler, M., and Stahl, K.: Catchment water storage variation with elevation, Hydrological Processes, 31, 2000–2015, https://doi.org/10.1002/hyp.11158, 2017.

Suecker, J. K., Ryan, J. N., Kendall, C., and Jarrett, R. D.: Determination of hydrologic pathways during snowmelt for alpine/subalpine basins, Rocky Mountain National Park, Colorado, Water Resources Research, 36, 63–75, https://doi.org/10.1029/1999WR900296, 2000.

Tague, C. and Grant, G. E.: Groundwater dynamics mediate low-flow response to global warming in snow-dominated alpine regions, Water Resources Research, 45, 1–12, https://doi.org/10.1029/2008WR007179, 2009.

Tague, C., Grant, G., Farrell, M., Choate, J., and Jefferson, A.: Deep groundwater mediates streamflow response to climate warming in the Oregon Cascades, Climatic Change, 86, 189–210, https://doi.org/10.1007/s10584-007-9294-8, 2008.

Veettil, B. K., Leandro Bayer Maier, E., Bremer, U. F., and de Souza, S. F.: Combined influence of PDO and ENSO on northern Andean glaciers: a case study on the Cotopaxi ice-covered volcano, Ecuador, Climate Dynamics, 43, 3439–3448, https://doi.org/10.1007/s00382-014-2114-8, 2014a.

Veettil, B. K., Maier, E. L. B., Bremer, U. F., and de Souza, S. F.: Combined influence of PDO and ENSO on northern Andean glaciers: a case study on the Cotopaxi ice-covered volcano, Ecuador, Climate dynamics, 43, 3439–3448, 2014b.

Veettil, B. K., Bremer, U. F., de Souza, S. F., Maier, E. L. B., and Simões, J. C.: Influence of ENSO and PDO on mountain glaciers in the outer tropics: case studies in Bolivia, Theoretical and Applied Climatology, 125, 757–768, https://doi.org/10.1007/s00704-015-1545-4, 2016.

Vermote, E.: MOD09A1 MODIS/Terra Surface Reflectance 8-Day L3 Global 500m SIN Grid V006, NASA EOSDIS Land Processes DAAC, 2015.

Vuille, M. and Bradley, R. S.: the tropical Andes, Geophysical Research Letters, 27, 3885–3888, 2000.

Vuille, M. and Keimig, F.: Interannual Variability of Summertime Convective Cloudiness and Precipitation in the Central Andes Derived from ISCCP-B3 Data, Journal of Climate, 17, 3334–3348, https://doi.org/10.1175/1520-0442(2004)017<3334:IVOSCC>2.0.CO;2, 2004.

Vuille, M., Bradley, R. S., Werner, M., and Keimig, F.: 20th Century Climate Change in the Tropical Andes: Observations and Model Results, in: Climatic Change, vol. 59, pp. 75–99, https://doi.org/10.1007/978-94-015-1252-7_5, 2003.

Vuille, M., Francou, B., Wagnon, P., Juen, I., Kaser, G., Mark, B. G., and Bradley, R. S.: Climate change and tropical Andean glaciers: Past, present and future, Earth-Science Reviews, 89, 79–96, https://doi.org/10.1016/j.earscirev.2008.04.002, 2008.

Vuille, M., Carey, M., Huggel, C., Buytaert, W., Rabatel, A., Jacobsen, D., Soruco, A., Villacis, M., Yarleque, C., Elison Timm, O., Condom, T., Salzmann, N., and Sicart, J.-E.: Rapid decline of snow and ice in the tropical Andes – Impacts, uncertainties and challenges ahead, Earth-Science Reviews, 176, 195–213, https://doi.org/10.1016/j.earscirev.2017.09.019, 2018.

Wagnon, P., Ribstein, P., Francou, B., and Sicart, J. E.: Anomalous heat and mass budget of Glaciar Zongo , Bolivia , during the 1997 / 98 El Ni · o year, Journal of Glaciology, 47, 21–28, 2001.

Wickert, A. D.: The ALog: Inexpensive, Open-Source, Automated Data Collection in the Field, The Bulletin of the Ecological Society of America, 95, 166–176, 2014.

Wilson, A. M., Williams, M. W., Kayastha, R. B., and Racoviteanu, A.: Use of a hydrologic mixing model to examine the roles of meltwater, precipitation and groundwater in the Langtang River basin, Nepal, Annals of Glaciology, 57, 155–168, https://doi.org/10.3189/2016AoG71A067, 2016.

Wosten, J. H. M., Lilly, A., Nemes, A., and Le Bas, C.: Development and use of a database of hydraulic properties of European soils, Geoderma, 90, 169–185, 1999.